Lethaia
AN INTERNATIONAL JOURNAL OF PALAEONTOLOGY AND STRATIGRAPHY

Palaeoenvironments, stratigraphy and taphonomy of an Upper Triassic vertebrate-bearing unit, Silves Group, central Algarve, southern Portugal

MACIEJ RUCIŃSKI, LOPE EZQUERRO RUIZ, HUGO CAMPOS, OCTÁVIO MATEUS, PAULO FERNANDES, MARGARIDA VILAS-BOAS, HAYTHAM EL ATFY AND INGMAR WERNEBURG

LETHAIA

Triassic to Lower Jurassic deposits known as the Silves Group in the Algarve, southern Portugal, have been studied for over 150 years. However, many of this unit's sedimentological, stratigraphical, and palaeontological aspects remain poorly documented. Here, we present novel observations on sedimentology, stratigraphy, taphonomy, and fauna at the Rocha da Pena site, located in the central part of the Algarve Basin. The investigated sequence is established to correspond to the upper part of the Silves Group. The mudstone, calcrete, and palustrine carbonate facies comprise most of the sequence thickness and are interpreted as having been deposited within coastal alluvial mudflats to palustrine settings under semi-arid and seasonal climates. The overlying siltstone and sandstone facies indicate an environmental shift towards tidally influenced environments, subsequently covered by the latest Triassic to earliest Jurassic volcaniclastics and basaltic lava flows. Furthermore, novel faunal elements, including actinopterygian and unionoid bivalves, are described from mudstone layers. New fossiliferous beds are identified within palustrine facies that yield numerous but poorly preserved materials assigned to cyamodontoid placodonts, hybodont sharks, and actinopterygians. The poor preservation of the remains is attributed to the pedogenetic processes prevalent in the palustrine depositional setting. A distinct faunal composition between the mudstone and palustrine facies is observed. It is preliminarily hypothesized to be likely linked with salinity fluctuations, but sampling bias cannot currently be excluded. The recovered vertebrate fauna aligns most closely with the Carnian and, to a lesser extent, the Norian fossil record. Nonetheless, the precise age of the fossil-bearing levels remains uncertain and can currently be reliably constrained to the upper Carnian–Rhaetian interval. Consequently, this work provides new insights into the palaeoenvironmental evolution of the western Tethys margin during the Late Triassic and highlights the relevance of the Silves Group in reconstructing coastal-continental ecosystem dynamics in southwestern Iberia. ☐ *Triassic-Jurassic palaeoenvironments, sedimentology, taphonomy, vertebrates, Portugal*

Maciej Ruciński ✉ [maciej.rucinski@nhm.uio.no], Natural History Museum, University of Oslo, P.O. Box 1172 Blindern, NO-0318 Oslo, Norway and GeoBioTec, Department of Earth Sciences, NOVA School of Science and Technology, Universidade Nova de Lisboa, Portugal; Lope Ezquerro Ruiz [lopezque@ucm.es], Departamento de Ciencias de la Tierra, Facultad de Ciencias Geológicas, Universidad Complutense de Madrid, 28040, Madrid, Spain; Hugo Campos [hugo.campos@geoparquealgarvensis.pt], Loulé Municipal Museum, Portugal and UNESCO Global Geopark Algarvensis, Portugal; Octávio Mateus [omateus@fct.unl.pt], *GeoBioTec, Department of Earth Sciences, NOVA School of Science and Technology, Universidade Nova de Lisboa, Portugal; Paulo Fernandes [pfernandes@ualg.pt], Centre for Marine and Environmental Research, University of Algarve, Campus de Gambelas, Faro, Portugal; Margarida Vilas-Boas [anamargarida.silvavilasboas@unipg.it], Dipartimento di Fisica e Geologia, Università degli Studi di Perugia, 06123 Perugia, Italy; Haytham El Atfy [el-atfy@daad-alumni.de], Palaeobotany Group, Institute of Geology and Palaeontology, University of Münster, Münster 48149, Germany and Geology Department, Faculty of Science, Mansoura University, 35516 Mansoura, Egypt; Ingmar Werneburg [ingmar.werneburg@senckenberg.de], Fachbereich Geowissenschaften der Universität Tübingen, Paläontologische Sammlung, Hölderlinstraße 12, 72074, Tübingen, Germany and Senckenberg Centre for Human Evolution and Palaeoenvironment an der Universität Tübingen, Sigwartstraße 10, 72076, Tübingen, Germany;* *manuscript received on 01/03/2025; manuscript accepted on 28/10/2025; manuscript published on 19/01/2026 in Lethaia 59*(3).

The Algarve Basin in southern Portugal constitutes a Mesozoic sedimentary basin encompassing the Silves Group, which preserves a rich record of Late Triassic to Early Jurassic faunal and floral remains (Brusatte *et al*. 2015; Palain 1976; Rocha 1976; Terrinha *et al*. 2019; Vilas-Boas *et al*. 2024). During the early Mesozoic, the Algarve Basin was positioned in central Laurasia, where significant biotic changes (Benton & Wu 2022) coincided with rifting phases that facilitated the westward expansion of the Neotethys Ocean (Terrinha

https://doi.org/10.18261/let.59.3.3

et al. 2019). This tectonic activity led to the opening of the Central Atlantic Ocean and the formation of the Central Atlantic Magmatic Province (CAMP), ultimately triggering the End-Triassic environmental changes, mass extinction, and the breakup of Pangaea (e.g. Davies *et al*. 2017; Marzoli *et al*. 1999; Panfili *et al*. 2019; Sues & Fraser 2010; Wignall & Atkinson 2020).

The fossil and geological record of the Silves Group in the Algarve Basin has the potential to clarify the palaeoenvironmental transitions and faunal evolution during this period of profound structural and biotic change. The Silves Group spans Upper Triassic continental siliciclastic deposits containing vertebrate fossils to Lower Jurassic shallow lagoonal carbonates and evaporites, which preserve invertebrate fauna (Brusatte *et al*. 2015; Mateus *et al*. 2014; Rocha 1976; Terrinha *et al*. 2019). Moreover, due to its palaeogeographical position at the southern Laurasian continental margin, near the contact of the Laurasian and Gondwanan landmasses, today represented by Europe, North America, and Africa, the Algarve Basin creates a worthwhile area for palaeogeographical and palaeobiogeographical studies (Brusatte *et al*. 2015).

Research on the Triassic deposits of the 'Grés de Silves' (= Silves Group) in the Algarve, southern Portugal, began in the 19th century (Bonnet 1850; Choffat 1887), and since then, numerous proposals for stratigraphical division, age, and palaeoenvironment interpretations have been presented (Azerêdo *et al*. 2003; Manuppella 1992; Palain 1968a; 1968b; 1976; 1979; Pratsch 1958; Rocha 1976; Teixeira 1942). Substantial attention has been directed to the study of the lower part of the Silves Group, represented by the Late Triassic sandstones and conglomerates (Arche & López-Gómez 2014; Dinis *et al*. 2018; Gama *et al*. 2021; Palain 1976; Pereira & Gama 2017; Pereira *et al*. 2017) containing palynomorphs (Vilas-Boas 2023; Vilas-Boas *et al*. 2022; Vilas-Boas *et al*. 2024), macrofloral (Teixeira 1948) and ichnological (Mayoral *et al*. 2016) records. In contrast, the overlying mudstone-carbonate and evaporite units that yielded vertebrate material (Brusatte *et al*. 2015; Mateus *et al*. 2014; Russel & Russel 1977; Witzmann & Gassner 2008) long had a less precisely constrained stratigraphy (e.g. Azerêdo *et al*. 2003; Brusatte *et al*. 2015; Vilas-Boas *et al*. 2024) and a relatively scarce amount of bed-scale sedimentological studies (Lopes 2014; Palain 1976; Russel & Russel 1977)

This study aimed to provide new insights and interpretations of the rock sequence corresponding to the vertebrate fossil-bearing parts of the Upper Triassic Silves Marl-Carbonate Evaporitic Complex, constituting the upper portion of the Silves Group. The deposits around the area of Rocha da Pena in Loulé municipality were selected for this study due to well-exposed, extensive outcrops and vertebrate fossil content (Brusatte *et al*. 2015; Lopes 2014; Mateus *et al*. 2014). The local stratigraphy is established, coupled with palaeoenvironment interpretations. Moreover, new fossil-bearing layers were identified during the study, yielding vertebrate fossil material. The sedimentological, palaeontological, and stratigraphical data are summarized, offering new insights into the stratigraphy and palaeoenvironments of the Upper Triassic strata of the Algarve Basin.

Geological setting

Algarve Basin

The Algarve Basin (Fig. 1A, B), constitutes the Meso-Cenozoic Southwest Iberia Margin of the Iberian microplate (Terrinha *et al*. 2019). The Basin extends around 140 km from the Cabo de São Vicente on the western coast of Portugal to the Guadiana River on the east (Terrinha *et al*. 2006). The basement of Algarve Basin (Fig. 1C, D) consists of the Variscan South Portuguese Zone, with low-grade metasedimentary, volcanic, and igneous rocks ranging in age from the Devonian to Carboniferous (Onézime *et al*. 2003; Jorge *et al*. 2013; Rodrigues *et al*. 2015; Pereira & Gama 2017).

The Algarve Basin originates from the post-Variscan divergent movements related to the opening and westward expansion of the Neotethys (Terrinha *et al*. 2019). During the Triassic (Fig. 1E, F), the rifting phase initially occurred along the Laurasia-Gondwana boundary between Iberia and Africa (Ramos *et al*. 2016; Terrinha *et al*. 2019). The subsequent expansion of the rifted area led to the opening of the North and Central Atlantic Ocean, initiating the breakup of Pangaea (Leleu *et al*. 2016; Ramos *et al*. 2016; Terrinha *et al*. 2019).

Sedimentation in the Algarve Basin started in the Late Triassic with the deposition of red beds unconformably over the folded and faulted Carboniferous turbidites of the South Portuguese Zone (Fig. 1C, D), corresponding to a hiatus of ca. 80 Ma (Terrinha *et al*. 2019; Vilas-Boas *et al*. 2022). At the end of the Triassic, rifting associated with the Pangaea breakup was accompanied by intense volcanism of the CAMP (Marzoli *et al*. 1999; Nomade *et al*. 2007). The CAMP extended from South America to Europe, covering approximately 11 million km^3, with well-recorded exposures in the Algarve Basin (Leleu *et al*. 2016; Martins *et al*. 2008; Pérez-López *et al*. 2021; Verati *et al*. 2007; Youbi *et al*. 2003).

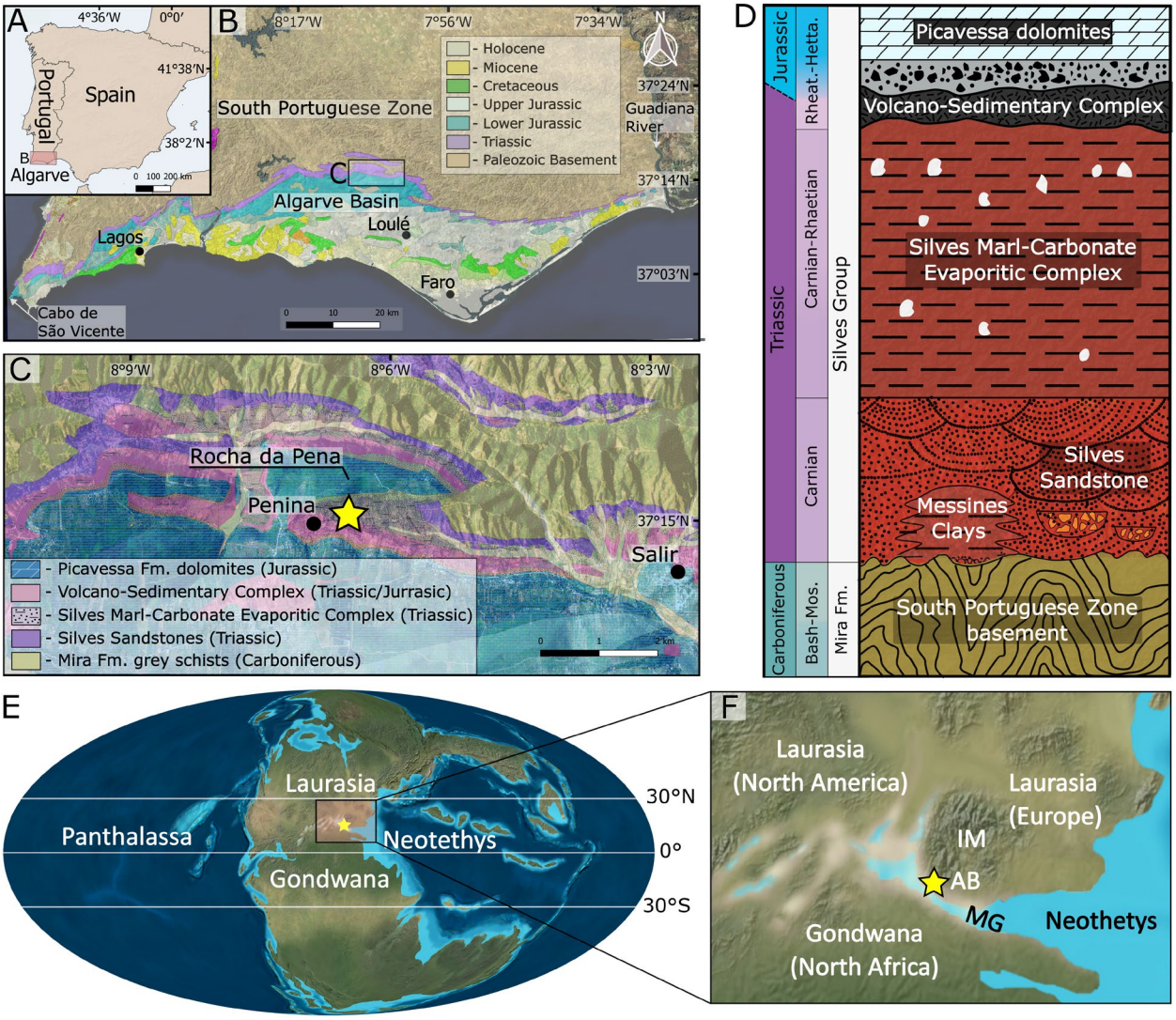

Fig. 1. Map and stratigraphical context of the Algarve Basin and locations investigated. A, an overview map of the Iberian Peninsula showing the location of the Algarve region. B, geological map of the Algarve region (modified from LNEG Carta Geológica Portugal 1:1 000 000, 2010). C, geological map of the studied area with the researched locality indicated by a yellow star (modified from LNEG Carta Geológica da Região do Algarve, 1:100 000, 1992). D, synthetic stratigraphy of the Silves Group in the area of the Rocha da Pena. Note that due to tectonic activity in the Algarve Basin, regional stratigraphical variations exist. For example, the thick evaporitic deposits observed at the top of the Silves Marl–Carbonate Evaporitic Complex, such as those associated with the Loulé and Albufeira diapirs, are absent north of the Algibre Fault (Vilas-Boas *et al.* 2024), thus in the area investigated. In the Rocha da Pena area, evaporites commonly occur as gypsum nodules, which are indicated on the log as white patches. E, palaeogeographical map illustrating Pangaea during the Late Triassic (Colorado Plateau Geosystems Inc., license no. #110719). F, enlarged map of the Late Triassic with a focus on the Iberian region. Yellow star indicates the position of the Algarve Basin. Abbreviations: AB - Algarve Basin, IM - Iberian Massive, MG - Maghrebian-Gibraltar rift.

The deposition of thick evaporite deposits, present solely south of the Algibre Fault (see Vilas-Boas *et al.* 2024, figs 1, 2) occurred at the Triassic–Jurassic boundary through the Hettangian and was coeval with the CAMP volcanism (Vilas-Boas *et al.* 2024). The last depositional phase was followed by a marine transgression recorded by mainly massive, fine crystalline dolomitic limestones and dolomites, marking the initiation of sedimentation on a passive margin carbonate platform that lasted until the upper Early Cretaceous (Albian) (Palain 1976; Rocha 1976; Terrinha *et al.* 2006). Sedimentation in the Algarve Basin resumed only in the Early Miocene with the deposition of bioclastic limestones of the Lagos-Portimão Formation, which unconformably overlaid the deformed Mesozoic strata. This deformation phase occurred during the Palaeogene when the collision of the Iberian Microplate and the African plate

caused the tectonic inversion of the Algarve Basin and formed the regional tectonic structures observed (Ramos *et al*. 2016; Terrinha *et al*. 2019).

The Silves Group

The Upper Triassic deposits outcrop in a primarily continuous, thin belt, a few kilometres wide, stretching from west to east throughout most of the Algarve region (Fig. 1B). These deposits have been attributed to the 'Grés de Silves' unit, which was established by Paul Choffat in 1887. Soares *et al*. (2007; 2012) proposed an alternative term, the Silves Group, as a synthetic unit encompassing the basal Mesozoic deposits of Portugal, including the Triassic to Lower Jurassic sediments of the Lusitanian and Algarve basins (Soares *et al*. 2007; Soares *et al*. 2012). Consequently, the early Mesozoic deposits of the Algarve Basin are referred to in the literature as 'Grés de Silves', Grés de Silves Formation or Silves Group, depending on the authors and time of publication. The stratigraphical delineation and division of the Silves Group deposits in the Algarve have been extensively debated, resulting in multiple interpretations (Choffat 1887; Manuppella 1992; Palain 1976; Palain 1979; Pratsch 1958; Rocha 1976). Among the interpretations of the Upper Triassic to Early Jurassic deposits in the Algarve Basin, the works of Palain (1976; 1979), Rocha (1976), and Manuppella (1992) have remained commonly referenced. The most recent advances in the Silves Group stratigraphy were presented in the palynological studies by Vilas-Boas *et al*. (2022; 2024), which constrain the age of stratigraphical units for the first time. According to a survey conducted by Manuppella (1992), followed by Vilas-Boas *et al*. (2022; 2024), the Silves Group consists of three principal units: (1) Silves Sandstones; (2) Silves Marl-Carbonate Evaporitic Complex; and (3) the Volcano-Sedimentary Series, which are herein adopted.

The lower-most unit of the Silves Sandstones, occurring only locally in the central Algarve, is termed *São Bartolomeu de Messines Clays* (Manupella 1992; Vilas-Boas *et al*. 2022; Vilas-Boas *et al*. 2024) or Unit AA *sensu* Palain (1976; 1979). It encompasses conglomerates at the base, followed by claystones and siltstones (Manupella 1992; Vilas-Boas *et al*. 2022; Vilas-Boas *et al*. 2024).

The succession of parallel or cross-bedded fine to coarse, mostly red sandstone, locally intersected by palaeochannels filled with conglomerate, is attributed to Silves Sandstones corresponding to AB1 term of Palain (1976;1979); '*Arenitos de Silves*' (together with previously mentioned underlying deposits) of Rocha (1976), and '*Grés de Silves*' unit of Manupella (1992). The unit has been construed to be Carnian in age (Vilas-Boas *et al*. 2022). The basal part of the Silves Sandstones is lower Carnian in age, while the upper part corresponds to the upper Carnian (Vilas-Boas *et al*. 2022; Vilas-Boas *et al*. 2024).

The sequence, composed of variegated, mostly red to green mudstones interbedded with siltstones, limestones, dolomites, and locally occurring fine sandstones and evaporites, constitutes most of the portion of Silves Marl-Carbonate Evaporitic Complex (Manupella 1992; Vilas-Boas *et al*. 2024), equivalent to AB2 term of Palain (1976, 1979). The unit has been constrained to the upper Carnian-lowermost Hettangian interval (Vilas-Boas *et al*. 2024)

The uppermost part of the Silves Group in the Algarve comprises discontinuous units of volcanic rocks associated with tuff and breccias, belonging to the Volcano-Sedimentary Series, which is lowermost Jurassic in age (Verati *et al*. 2007; Vilas-Boas *et al*. 2024).

Study area and methods

Our stratigraphical study comprised a detailed log and correlation of four profiles located along the Rocha da Pena and Vale do Álamo areas, close to Penina locality (Fig. 1C), that encompass a combined 28 m thick sedimentary sequence (Fig. 2). The profiles were roughly made following a transect, trending approximately NW-SE, with an average spacing of 200 m between each other (Fig. 2). They were named, from north to south, as belonging to Rocha da Pena (RP1 and RP2) or Vale do Álamo (VA1 and VA2), respectively (Figs 2, 3). The study also involved sedimentological analysis, including identification and interpretation of lithofacies and facies associations according to classical criteria (lithology, texture, geometry of sedimentary bodies, sedimentary structures, fossil content). The study was completed with thin sections to characterize the structure and texture of the sediments at the mm-scale, which were performed at the Servicio de preparación de rocas y materiales duros of the University of Zaragoza and photographed using an optical petrographical microscope Olympus BX41 mounted with PROMICAM PRO 3-3CP camera.

Fossil samples were found in and collected from isolated blocks, with a smaller portion of specimens recovered directly from the mudstone or carbonate beds. The samples were prepared at Departamento de Ciências da Terra da Faculdade de Ciências e

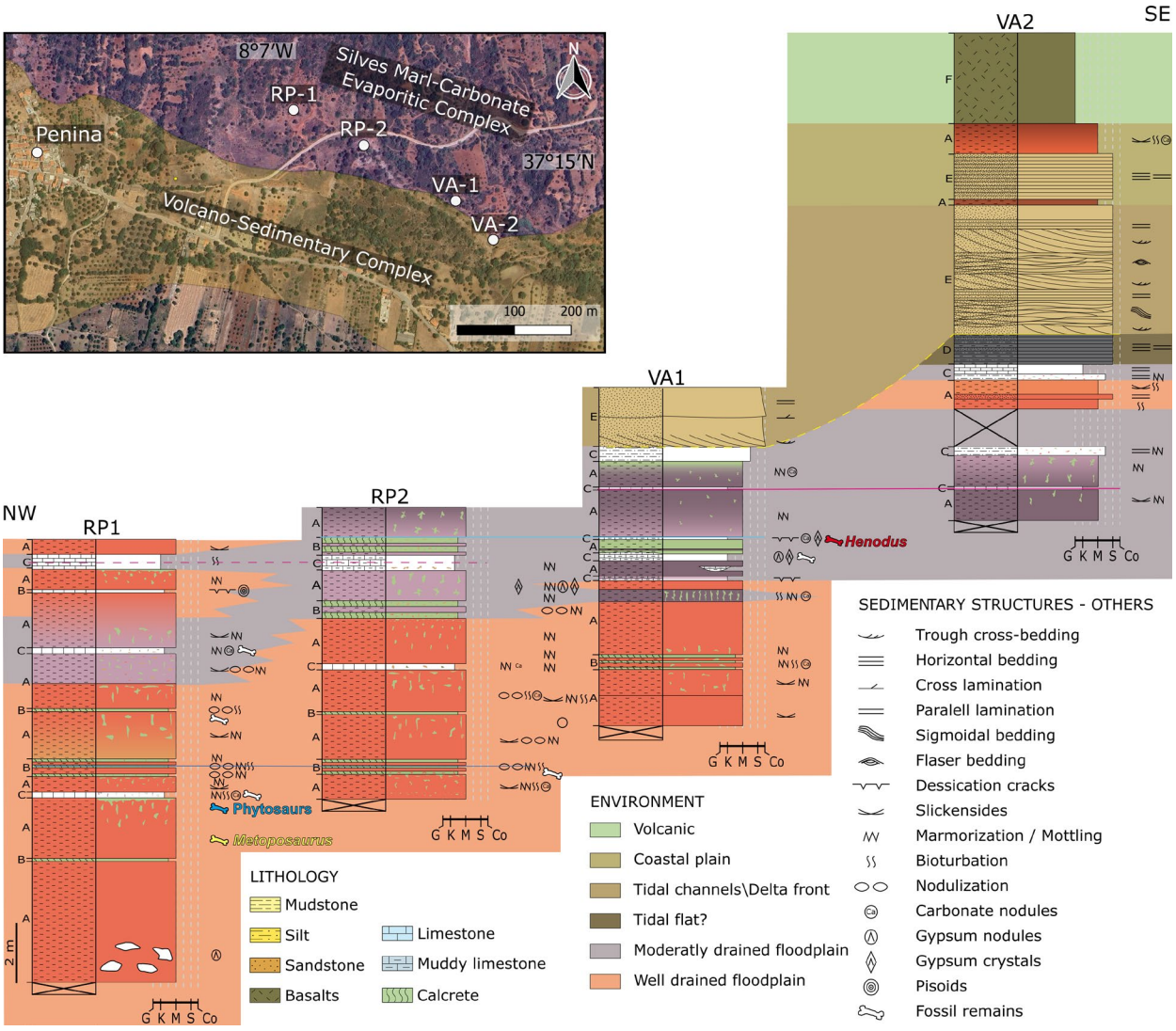

Fig. 2. Sedimentary log of successions near Penina; the map illustrates the location of studied sections. Capital letters A to F correspond to the facies associations.

Tecnologia da Universidade Nova de Lisboa. Paraloid B-72 diluted in acetone was used as a consolidant and glue. All specimens presented in this study are housed at the Departamento de Ciências da Terra da Faculdade de Ciências e Tecnologia da Universidade Nova de Lisboa.

Maps were created in QGIS (v.3.28), using the geological map modified from LNEG Carta Geológica Portugal 1:1 000 000, 2010, and from LNEG Carta Geológica da Região do Algarve, at a scale of 1:100 000, 1992. Specimens were photographed with a Canon EOS 50D camera. The photographs and illustrations were compiled into figures using Inkscape (v.1.3.2).

An aliquot of approximately 10 to 15 g per three claystone and calcrete samples from the base and top of RP2 and VA1 sections was prepared using traditional acid treatment maceration techniques, including cold HCl and HF, with no alkaline or oxidation processes (e.g. Riding 2021). After neutralization, the residues were sieved through a 10 µm nylon mesh. After sieving, all residues were separated via gravity separation using sodium polytungstate. Subsequently, the samples with the expected palynomorphs were strew-mounted on glass slides using glycerin gelatin. The mounted slides were viewed under transmitted white light and incident fluorescence microscopy. Unfortunately, no organic particles could be detected in any sample.

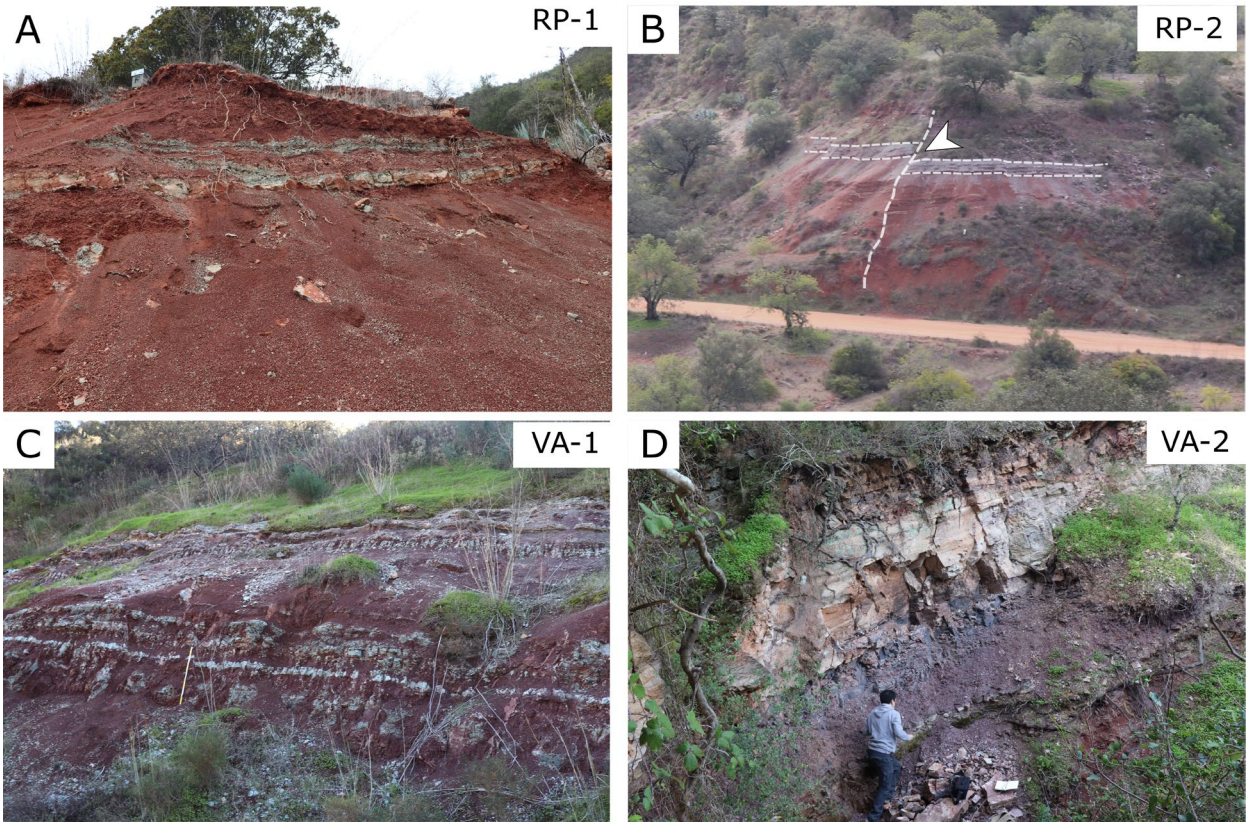

Fig. 3. Field photos of the studied outcrops near Penina, Loulé municipality. A, mudstone-carbonate unit exposed at the RP - 1 section composed of mudstone, calcrete, and palustrine facies. *Metoposaurus algarvensis* bonebed outcrops at this section. B, mudstone-carbonate unit exposed in the RP - 2 section. Note distinct deformations linked to syn-sedimentary rifting extensional faults as previously described in the Algarve Basin by Ramos *et al* (2016). C, middle portion of the mudstone-carbonate complex is exposed in the VA – 1 section. D, lower portion of the VA-2 section with outcrops of laminated calcareous silty mudstone and cross-bedded and laminated calcareous silty-sandstone facies. The upper portion of the section is depicted in below (Figs 8, 9).

Facies associations

The sedimentological analysis of the Rocha da Pena and Vale do Álamo outcrops enabled the establishment of six facies associations. The main characteristics are summarized in Table 1, and are discussed below.

Mudstone facies (Facies A)

Description.– Mudstone facies consist of tabular beds (dm- to m-thick) of massive reddish and purple mudstone beds with occasional green calcrete intercalations (cm- to dm-thick). Within the basal part of the RP1, RP2 and VA1 profiles (up to ~15 m), most of the mudstones are dark red to brown with light greenish laterally continuous intercalations (Fig. 4A). In the middle and upper part of these sections, the mudstones are variable in colour, ranging from brownish or dark purple to light green.

Most beds are characterized by various degrees of colour mottling, which is most evident in the lower and middle parts of the RP and VA profiles. Red to brown deposits exhibit pervasive light brown or light green/grey mottling (Fig. 4A, B). At the same time, dark purple mudstones are characterized by grey and olive mottling (Fig. 4C). The mottling presents different patterns such as subparallel stratified small patches, large chaotic masses, and sub-vertical shapes (rhizoliths), which increase in density upwards (Fig. 4A). Within the matrix, carbonate nodules, usually of mm-size, commonly occur. The relatively large (0.1 to 0.3m in diameter) gypsum nodules are rare and occur prevalently within the red mudstone matrix at the base of the RP1 section (Fig. 4D). At the microscale, filled-porosity of gypsum has been recognized. Microcracks and slickensides are common in most mudstones, though their prevalence and size vary between beds. They are straight, concave, or elongated, often filled with secondary

Table 1. Description of sedimentological and microfacies features of facies associations recognized in the Rocha da Pena area and interpretation of sedimentary processes leading to their deposition

Lithofacies	Sedimentological and microfacies features	Sedimentary processes
Massive mudstones **Facies A**	Tabular beds; red, brown, purple to light green; various degrees of blocky cleavage; colour mottling, slickenside structures; calcium carbonate and gypsum nodule.	Mud deposition from suspension in low-energy environments (standing water) and\or from suspended load from waning flood flows; development of soil from mud sediments under variable drainage conditions.
Calcretes **Facies B**	Tabular or undulated beds; prismatic structure or patches of carbonate in mudstone matrix; colour mottling; nodulization; rhizotubules; rhizoconcretions; occasional desiccation cracks and rosettes at the top of bed. *Peloidal microspar; residual fissured micrite and mudstone; locally drusy cement.*	Advanced soil development from mud sediments under variable drainage conditions and dense vegetation cover (represented by beds with rhizotubules and rhizoconcretions).
Palustrine carbonates **Facies C**	Tabular beds; grey to white; locally marmoratization; desiccation and syneresis cracks; in selected beds brecciation. *Predominantly wackestone; more seldomly packstone and mudstone; peloidal microspar with patches of residual micrite; some beds with intraclasts and vadose cements.*	Calcium carbonate precipitation in shallow perennial water bodies within low-gradient terrain; sub-aerial to aerial exposure and pedogenesis.
Laminated calcareous silty mudstones **Facies D**	Tabular beds; lamination; pale grey-blue, red and dark laminae; laminae horizontal and undulated; variable degree of calcium carbonate cementation. *Microspar and peloidal microspar framed by laminae of micrite and mudstone; spheroids.*	Deposition by suspension in a low-gradient setting and prevalently low-energy environment; tidal influence or variable degree of fluvial discharge; in situ calcium carbonate accretion by calcifying microbial communities.
Cross-bedded and laminated calcareous silty-sandstones **Facies E**	Tabular or slightly erosive bodies; white, grey to pale brown; silt to fine-sand sized grains; parallel lamination; flaser-bedding; trough cross-bedding; sigmoidal cross-bedding *Interlaced laminae of planar to undulated dark micritic and calcareous silt and fine sand Qz and Cbt grains; spheroids*	Deposition under tidally-influenced and variable flow regimes; from lower (parallel lamination), highly fluctuating (flaser bedding) and high energy environments (trough cross-bedding); migration of dunes (trough cross-bedding, sigmoidal cross-bedding).
Volcanoclastic and volcanic facies **Facies F**	Tuff occurring together with lutites; black, grey; pale yellow, pale green, dark brown; clast-supported peperite with brecciated basalts and volcanoclastic matrix; convoluted base; basaltic pseudobreccia.	Deposition during pyroclastic or phreato-magmatic flow (tuff); lava flows contacting water bodies and\or unconsolidated sediment (peperite); lava flows within the coastal plain (basalt pseudobreccia).

carbonate or evaporite, and range from a few centimetres to 0.5 m in length (Fig. 4C). In the middle part of the RP1 profile, unionid bivalves (this work) as well as remains of *Metoposaurus* and phytosaurs were recovered (Brusatte *et al*. 2015; Mateus *et al*. 2014).

Interpretation.– The prevalent reddish and brownish colours of the mudstones indicate oxidising conditions resulting from the weathering of ferromagnesian minerals (Bahr *et al*. 2020; Debret *et al*. 2011; Milroy *et al*. 2019; Vollmer *et al*. 2008). Mottling may occur due to redoximorphic conditions that lead associated with water movement through soil, creating an irregular distribution of iron and forming depleted iron masses (Pimentel *et al*. 1996; Retallack 2008; Tucker 2001; Turner 1980). The high carbonate content, along with a red mudstone matrix featuring green depletion zones and the low brownish-yellowish mottled content linked to the goethite (in green zones), indicates efficient drainage (Mack *et al*. 1993; Kraus & Hasiotis 2006). The purple mudstones with increased brownish mottling (goethite) represent moderately to poorly drained conditions (Mack *et al*. 1993; Pimentel *et al*. 1996; Kraus & Hasiotis 2006; Costantini *et al*. 2006; Retallack 2008).

Slickenside structures and micro-cracks are associated with high plasticity and a hydrophilic origin, resulting in the swelling of clay sediment during wet periods and shrinking in dry conditions (Gray & Nickelsen 1989; Reading 1996; Tabor & Myers 2015). Carbonate and evaporitic nodules also suggest a high

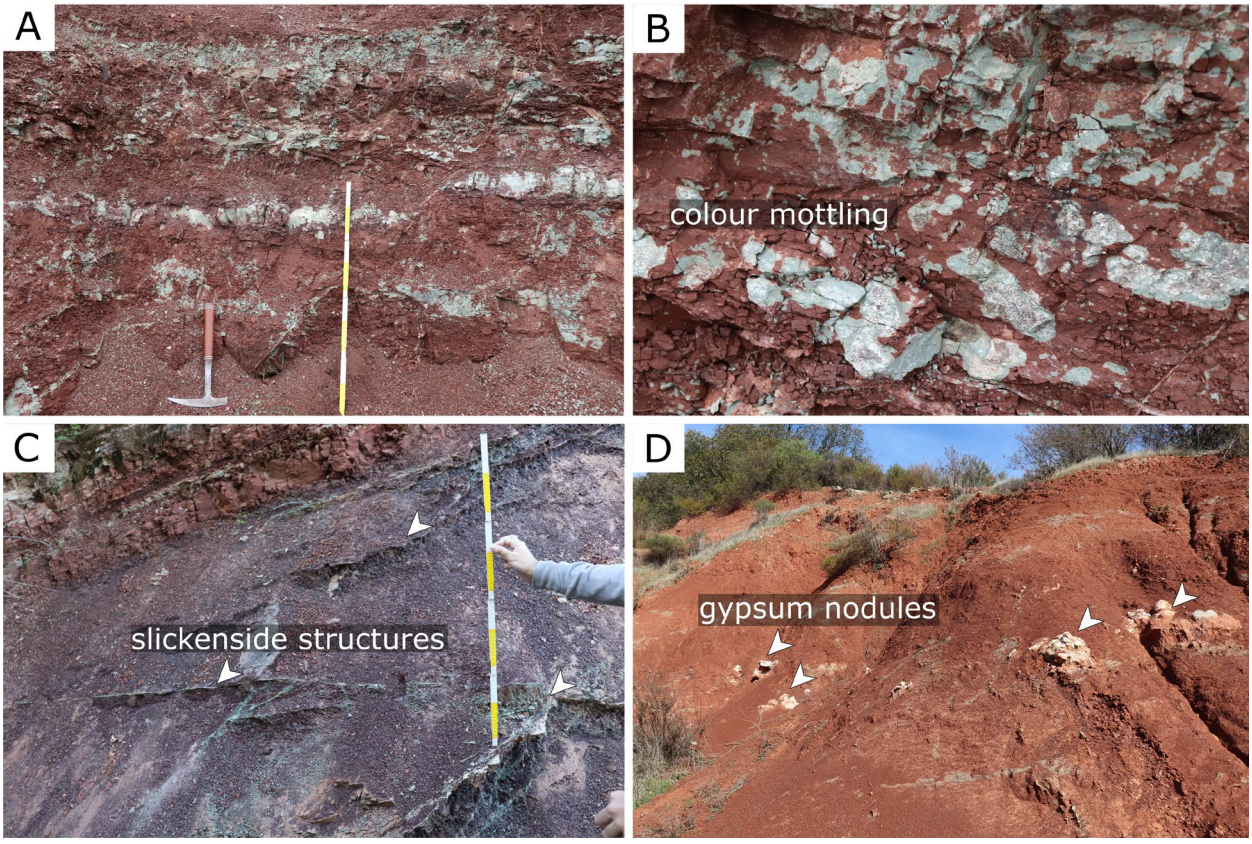

Fig. 4. Mudstone facies. A, photograph of red mudstones exhibiting pedogenetic features like colour mottling (occurring as subparallel stratified patches, chaotic masses, and sub-vertical shapes) and slickenside structures. B, colour mottling, grey-blue irregular mudstone patches within the red mudstone matrix. C, purple grey-green mottled mudstone with slickenside structures filled with secondary precipitated evaporites. D, red mudstones with the gypsum nodule-rich level outcropping near the *M. algarvensis* bonebed.

evaporation rate during certain times when the soil was dried and enriched with a saline fraction.

The sedimentological features of facies A, such as colour mottling, slickenside structures, and the formation of carbonate/evaporite nodules, are characteristic of deposits subjected to pedogenetic processes in semiarid to arid environments (Reading 1996; Retallack 2008; Tabor & Myers 2015; Tanner & Lucas 2006). These palaeosol profiles correspond to alternating Bw-Bwk horizons. Considering the low degree of superposition of characteristics, the soil profiles are predominantly composite palaeosols, although some compound profiles exist, indicating rapid and episodic sedimentation events (Retallack 1988; Kraus 1999).

Calcrete and calcareous mudstone facies (Facies B)

Description.– The calcrete facies are thin beds (usually 0.1 to 0.3 m thick) with nodular or prismatic structures interbedded with mudstone bodies. The contacts between the calcretes and mudstones vary from planar to irregular, with locally doming-upward structures at the top of the calcrete beds. Calcretes with prismatic structure comprise elongated and columnar carbonate nodules, often coalescent, developed primarily on red or purple matrix (Fig. 5A). Nodular calcretes are composed of spherical carbonate nodules developed in green to purplish mottled mudstone matrix, containing patches of calcareous mudstone (Fig. 5B). Parallel laminae or crusts appear at the top of the levels enriched in calcium carbonate. Fenestral porosity, nodulization, green rhizotubules and mottling, occasionally coating the rhizotubules, are common. Desiccation cracks, evaporitic nodules and rosettes appear at the top of some beds (Fig. 5C). In the microscale, one of the calcrete layers is composed of patches of strongly fissured residual micrite and phreatic cement represented by peloidal microspar (Fig. 5D). Drusy cement also occurs but is restricted to the filling of the large pores.

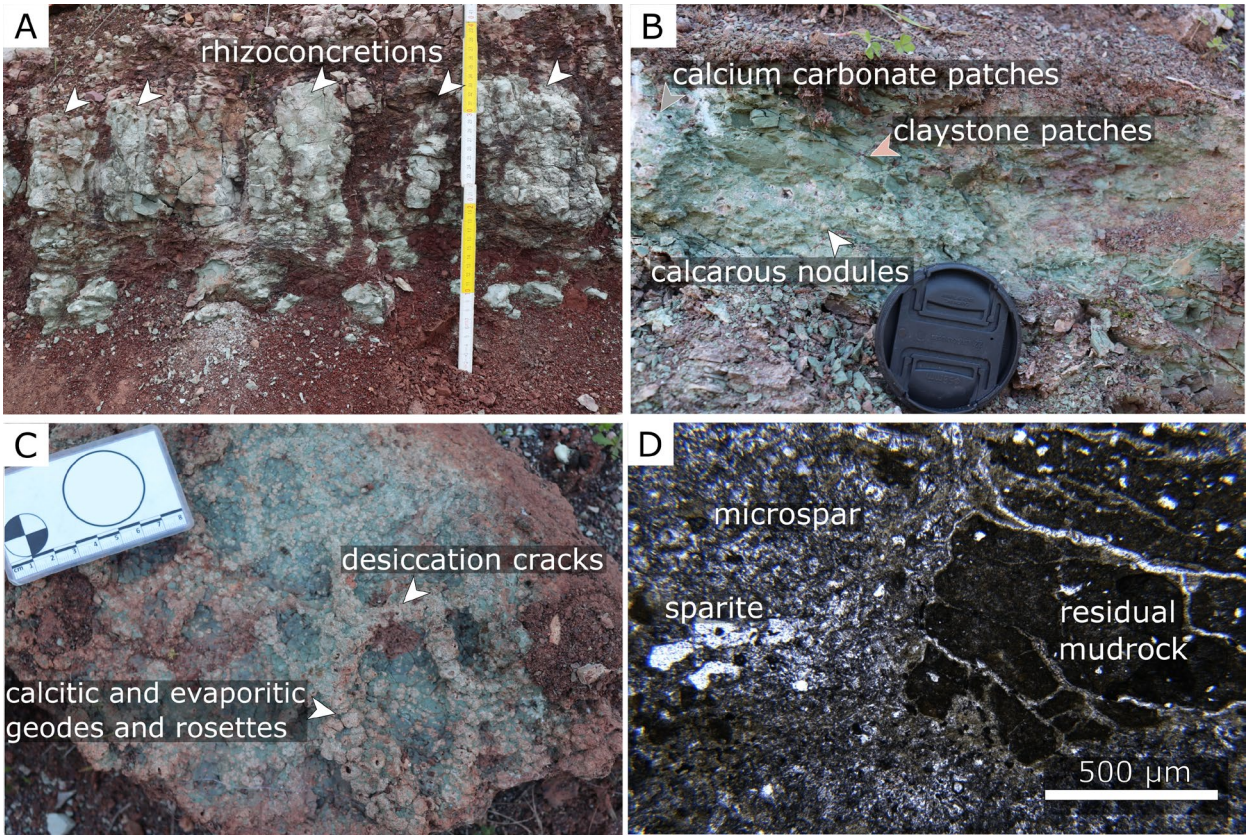

Fig. 5. Photos of calcrete and calcareous mudstone facies. A, calcrete with prismatic structure created by elongated columnar rhizoconcretions and purple mudstone matrix. B, pedogenetically modified calcareous mudstone exhibiting irregular carbonate concentration, resulting in carbonate-rich and non-cemented clay patches. Small (a few mm) calcareous nodules commonly occur within the layer's extent. Numerous isolated and often fragmented vertebrate fossils are present in this bed. C, top of the isolated block of calcareous mudstone layer with desiccation cracks and calcite and evaporitic geodes, often formed as local concentrations, sometimes following the shapes of desiccation cracks. D, photomicrograph of calcareous mudstone with a fissured block of residual mudstone and dominant microspar cement.

The middle part of the VA1 profile highlights a calcrete layer that contains numerous isolated and fragmented vertebrate fossils, mostly fish scales and reptilian bones.

Interpretation.– A considerable accumulation of calcium carbonate in various forms (chalky patches, nodules, aggregates and veins) within the mudstone matrix, coupled with colour mottling and rhyolites, is identified as calcretes (Alonso-Zarza 2003; Alonso-Zarza & Wright 2010; Reading 1996; Watts 1978).

Elongated carbonate nodules with a sub-vertical distribution, surrounded by the original red or purple matrix and exhibiting a high coalescence, correspond to rhizoconcretions. (Alonso-Zarza 1999; Klappa 1980; Kraus & Hasiotis 2006). Similar calcretes with the prismatic structure were often identified as well-developed calcisol, forming well-defined Bk or K horizons (e.g. Breda & Preto 2011; Dubiel & Hasiotis 2011; Marriott & Wright 2006; Retallack 1988; Mack 1993). The occurrence of this horizon suggests at least a temporary well-developed vegetation cover and root activity. The green colour of nodules and the mottled surrounding by a red or brownish colour indicate iron-depleted zones and well-drained conditions (Kraus & Hasiotis 2006; Pimentel *et al.* 1996). Probably, oscillations related to the near-surface water level in mudflats favoured the instauration of vegetation during wet periods and the genesis of carbonate nodules in drier episodes. The calcretes formed by spheric nodules and irregularly distributed patches of calcareous mudstone represent moderate to poorly drained conditions and likely shorter subaerial exposure (Alonso-Zarza 2003).

Palustrine carbonate facies (Facies C)

Description.– The palustrine carbonate facies consists mostly of massive, grey to white beds with

reddish and purplish mottling (Fig. 6A, B). The carbonates are predominantly wackestone in texture, transitioning locally into mudstone and packstone textures, occasionally exhibiting silty levels (Fig. 6C). Wackestone carbonates are mainly composed of peloidal microspar with variable-size patches of residual micrite, which is often strongly fissured (Fig. 6D). Clotted micrite texture occurs locally (Fig. 6E). Some of the palustrine beds represent brecciated limestone with micritic intraclasts with vadose cement (Fig. 6F). Facies C is characterized by a variable degree of porosity, which is mostly vug or breccia type. Desiccation cracks and, more commonly, syneresis cracks occur at the top of the beds. These layers often show brecciation features. Gypsum rosettes locally cover the top of some of the beds. Isolated patches of blocky sparite occur around the pores or fractures. Carbonate layers often contain isolated fish scales and bones, such as fragments of ribs and placodont armour plates.

Interpretation.– Several sedimentological features, such as brecciation, bioturbation, mottling, syneresis cracks, micrite intraclasts, and residual fissured micrite patches, suggest carbonate precipitation in shallow ponds and subsequent subaerial exposure (Alonso-Zarza 1999; Alonso-Zarza 2003; Freytet & Verrecchia 2002; Jewuła *et al*. 2023).

A large variability of both micro- and macrofabrics of these facies likely relates to the different degrees of transformation of the carbonates by the pedogenetic processes. The degree of pedogenesis ranges from poorly transformed deposits, such as: (1) mudstone texture with locally occurring clotted fabric; (2) most commonly occurring moderately affected wackestones; to (3) highly modified brecciated beds with mostly vadose cement. This textural variability reflects the influence of distinct early diagenetic environments across the palustrine beds. Some layers exhibit blocky to mosaic sparite cements (Fig. 6E), which are characteristic of phreatic diagenetic conditions, while some beds exhibit meniscus cements (Fig. 6F), pointing to vadose diagenesis (Alonso-Zarza 2003; Flügel & Munnecke 2010; Freytet & Verrecchia 2002). In some beds, the co-occurrence of multiple cement generations, ranging from micrite, microspar to mosaic spar and peloids, within individual samples indicates that these beds underwent complex, multi-phase cementation histories (Alonso-Zarza 2003; Freytet & Verrecchia 2002). Such overprinting suggests shifts in early diagenetic conditions, likely driven by fluctuations in the water table, episodes of subaerial exposure, and changes in pore-water calcium carbonate saturation (Alonso-Zarza 2003; Freytet & Verrecchia 2002). The occurrence of brecciation, both on a micro- and macroscale, may relate to mechanical and chemical processes as a consequence of wetting-drying cycles, leading to oscillating volume changes within the sediment, and resulting in the formation of autochthonous 'auto-breccia' (Alonso-Zarza 2003; Gierlowski-Kordesch 2010).

The facies C association represents shallow-water bodies in a temporal setting, where carbonates were formed in low-energy, low-gradient depositional settings within wetlands, lakes, or lagoon margins (Alonso-Zarza 2003). These water bodies were subjected to either episodic evaporation or regression during arid stages of the lower water table (Alonso-Zarza 2003; Jewuła *et al*. 2023; MacNeil & Jones 2006; Platt & Wright 1992; Platt & Wright 2023). Under those low-water conditions, the surface was subaerially exposed, enabling the desiccation (Alonso-Zarza 2003; Freytet & Verrecchia 2002).

Laminated calcareous silty mudstone facies (Facies D)

Description.– Laminated calcareous silty mudstone facies are exclusively exposed in the upper section of the Vale do Álamo site, consisting of planar millimetre-thick repeatedly interlayered pale grey-blue (2-10 mm), red (1-3 mm), and dark (< 1mm) parallel laminae, occasionally intercalated with fine-grained sandstones (Fig. 7A, B). Despite the dominant planar geometry, they are sometimes undulated, leading to locally occurring wavy bedding. Pervasive fenestral and fracture porosity have been observed, and sediment disturbances are evident as slightly undulating vertical channels.

The facies D displays layers with variable degree of lithification, from poorly consolidated calcareous silty mud, passing by well-consolidated with faintly marked conchoidally fractured blocks, to silty and muddy beds exhibiting fissility (Fig. 7A). At microscale laminated silty mudstones are composed of discontinuous laterally elongated laminae or fenestra (Fig. 7C). Those microspar laminae/fenestrae sometimes contain elongated and branching filaments of micrite. Isolated spheroid structures are common within both micrite and sparite laminae (Fig. 7C). They exhibit polygonal opaque crystals arranged in aggregates. Some of them are hollow, and the irregular internal surface and holes contain elongated and branching filaments of micrite or sparite (Fig. 7D).

Interpretation.– Finely laminated sediments indicate deposition in a low gradient and low-energy depositional environment. The rate of carbonate precipitation

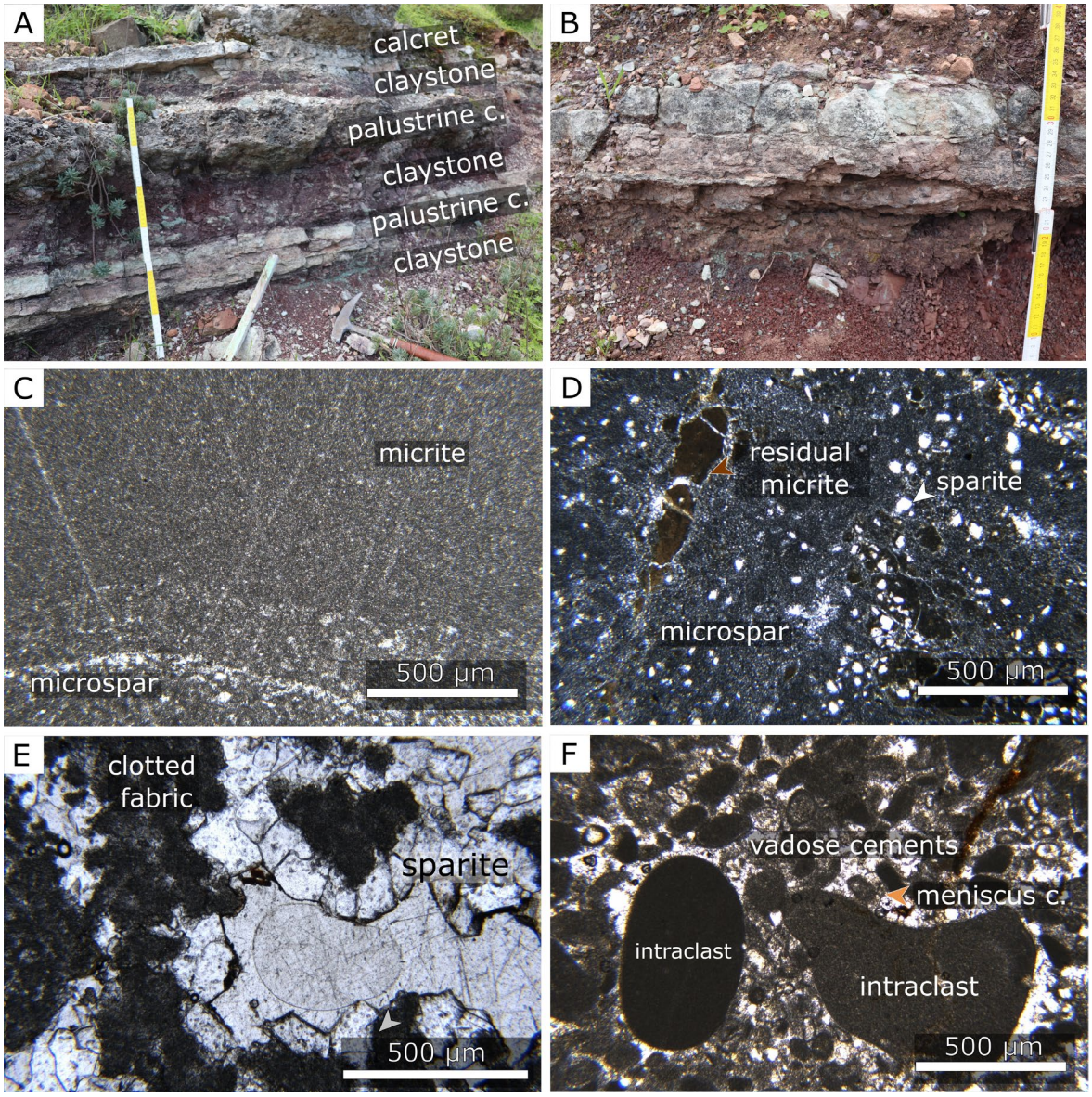

Fig. 6. Palustrine carbonate facies. A, photograph of intercalated palustrine carbonates, mudstones and calcrete, which constitute the most commonly observed facies association in the studied area. B, thin layer of palustrine carbonate with signs of limited brecciation and colour mottling. C, photomicrograph of palustrine carbonate representing mudstone texture with dominant micrite and locally occurring accumulations of microspar. D, photomicrograph of carbonate with fissured residual micrite patches with dominant microspar cement with dispersed calcitic sparite crystals. E, photomicrograph of carbonate with micritic clotted fabric and mosaic sparite. F, photomicrograph of brecciated limestone with micritic intraclasts and vadose meniscus and circumgranular cements.

varied as indicated by varying degrees of carbonate cementation. However, it was sometimes almost constant, as suggested by the laminated carbonate bed, indicating a permanent water body with common detrital (fine sand, silt and mud sizes) supplies (Braithwaite 2023; Vieira *et al.* 2019). The occurrence of laminated and undulated microstructures, micrite-aggregating clotted fabric, peloids, and fenestral porosity strongly suggests microbial activity in those deposits (Flügel & Munnecke 2010). Microbial activity can also be supported by the common occurrence of spheroids (Popa *et al.* 2004; Sawlowicz 1993; Sawlowicz 2000).

Due to observed features in Facies D and the clear tidal signal in the overlying Facies E, rhythmites might indicate a connection to tidalites (Kvale 2012; Mazumder & Arima 2005). However, due to the absence of direct marine\brackish indicators, the assertion of this interpretation will require further study. In these settings, the mudstone beds might have been deposited by suspension during

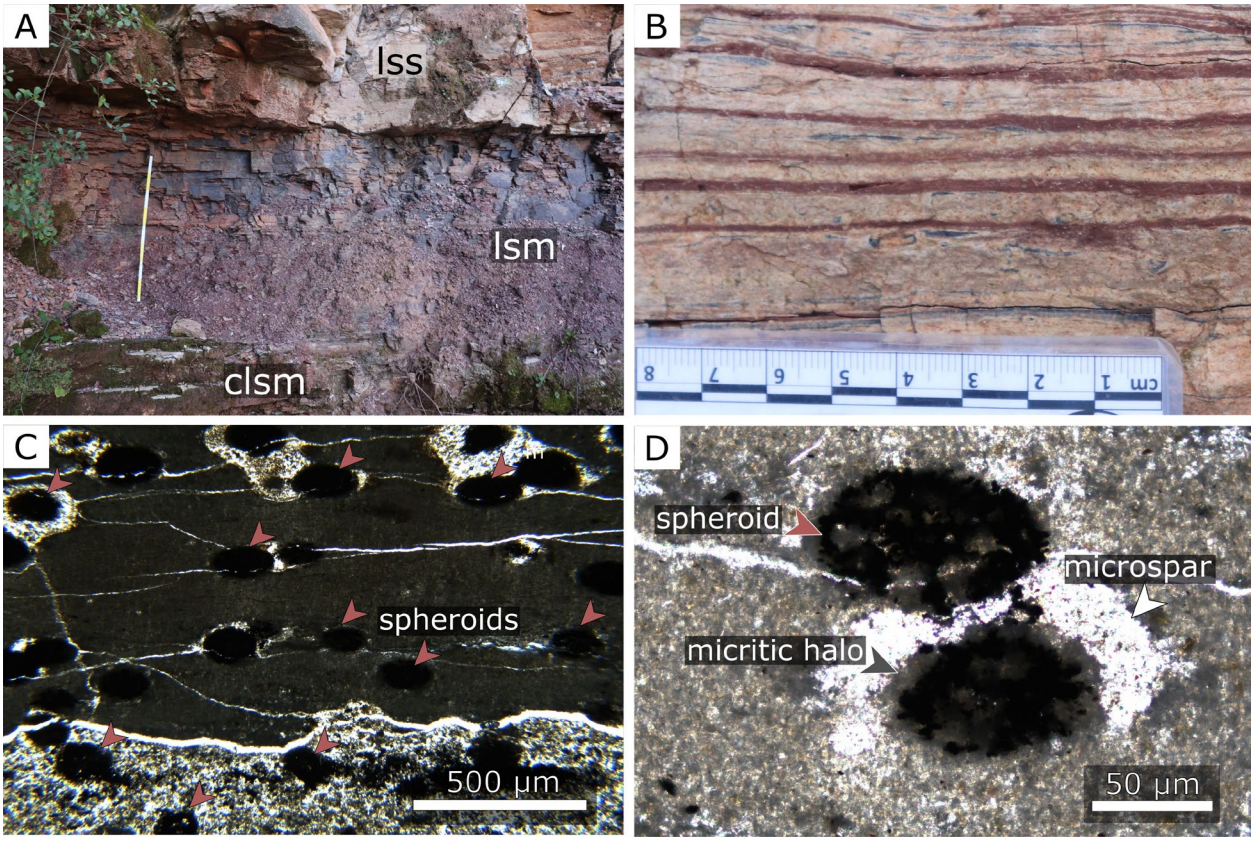

Fig. 7. Laminated calcareous silty mudstone facies. A, photograph of different types of laminated silty mudstone facies (clsm - calcareous laminated silty mudstones, characterised by strong calcium carbonate cementation; lsm - laminated silty mudstones with lower content of calcium carbonate, exhibiting a moderate degree of fissility; lss - laminated silty-sandstone facies). B, laminated calcareous silty mudstone with rhythmic beige, red and brown, predominantly planar to slightly undulating laminae. C, photomicrograph of laminae of calcareous silty mudstone. Fissured dark micritic laminae contain dark spheroids (examples indicated by red arrows) and contact the laminae, mainly composed of Qtz and calcareous silt-sized grains. D, spheroids are composed of opaque aggregates, surrounded by micritic halo and microspar.

high slack and low slack, whereas currents formed the silty and sandy beds during flood and/or ebb tide periods (Davis 2012). Alternatively, observed rhythmites might relate to oscillating degrees of sediment discharge with mudstone beds deposited by suspension, whereas the silty and sandy beds formed during episodes of more energetic flow and higher sediment influx (Milroy *et al.* 2019; Mulder & Alexander 2001).

Cross-bedded and laminated calcareous silty-sandstone facies (Facies E)

Description.– Within the studied localities, calcareous silty-sandstone facies are only represented by a ~7m thick body in Vale do Álamo sections (Fig. 8A), but they occur locally in the studied area as relatively thin, up to 2 m thick beds, generally at the top of the outcrops VA1 and VA2. Facies E is usually white or light grey, with a light brown weathered surface. They form poorly defined, coarsening-upwards beds with tabular or slightly erosive geometries, commonly presenting cross-bedding, parallel lamination, and dm-thick sets. Trough cross-bedding appears towards the bases with channelled geometries, grading upward in sigmoidal-cross stratification (Fig. 8A-C). Mud-draped ripples are observed in those layers (Fig. 8B, C). These beds are overlaid by flaser and wavy bedding in light brown to beige siltstones and dark mudstones, respectively (Fig. 8D). Locally, planar lamination alternates with them.

At the microscale, the Facies E is composed of planar to undulated silt to fine-grained quartz and carbonate grains, intercalated with dark micritic laminae (Fig. 8E). Spheroids, similar to the ones seen in laminated silty-mudstone facies D, occur mainly within the dark laminae.

Interpretation.– Silty-sandstone facies indicate a higher energy depositional environment characterized by channels (Ambrosetti *et al.* 2017; Davis 2012). Well-developed trough cross-stratification, convex upward geometries and slight erosional

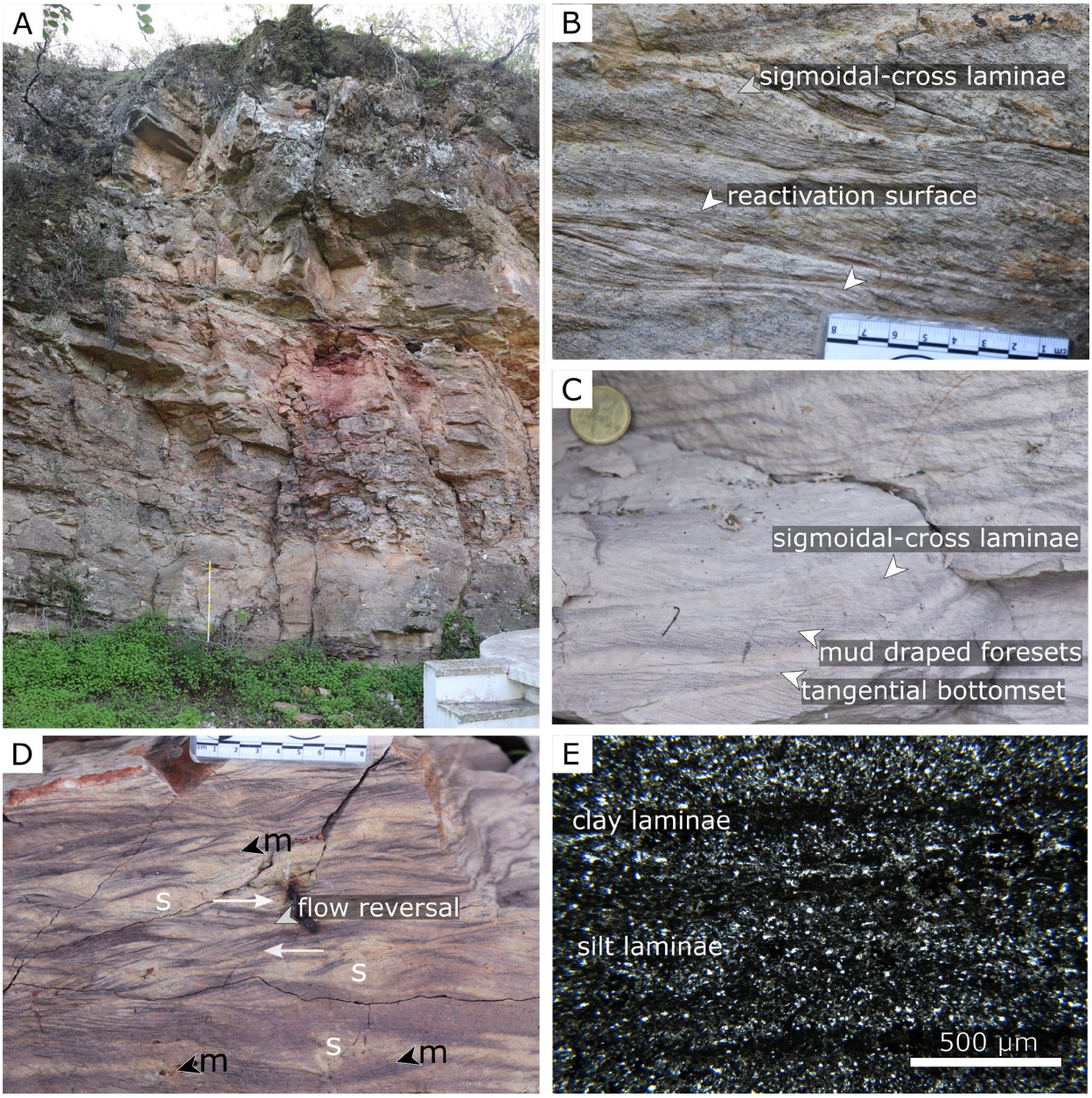

Fig. 8. Cross-bedded and laminated calcareous silty-sandstone facies exposed in the VA - s section. A, photograph of the thickest exposure of cross-bedded and laminated calcareous silty-sandstone in Vale do Álamo. B, sigmoidal cross-beddings visible near the bottom of a thick silty-sandstone at the Vale do Álamo succession, characterized by long sigmoidal laminae and reactivation surfaces indicating tidal bundles. C, sigmoidal cross beds with mud-draped foresets and tangential bottomsets observed near the bottom of a thick silty-sandstone succession, Vale do Álamo. D, flaser bedding composed of cross-bedded dark mud drapes within the yellowish siltstone. Examples of flow reversal are present in flaser-bedded layers. E, Photomicrograph of calcareous silty sandstone with Qtz and calcareous grains and poorly defined dark mud laminae. Spheroids similar to those observed in laminated calcareous silty mudstone facies are present but occur less frequently.

surfaces of shallow topographical relief represent channelled streams. The parallel laminated beds suggest tractional deposition from waning low-density flows. Flaser and wavy bedding indicate fluctuations in the rate of transport and supply of sediment, most likely a consequence of tidal influences (Pasierbiewicz 1982; Reineck & Wunderlich 1968; Wang 2012). The fine interlamination of sandstones and mudstones and the occurrence of mud-draped ripples are interpreted to be likely linked to tidal cycles (Davis 2012; Mellere *et al.* 2017; Visser 1980). Sigmoidal cross-stratification may occur in various environments, including fluvial, mouth bar and tidally-influenced settings and is related to

processes involving traction and fall-out processes, related to bypass and oscillation in combined flow, respectively (Tinterri 2011). In the case of the Vale do Álamo section, the presence of mud laminae and lateral variation in density of ripple accretion suggests tidal origin, thus a relation to tidal bundle and migration of subaqueous dunes (Davis 2012; Martinius 2012).

Facies E represents a higher-energy depositional environment influenced by both unidirectional and tidal currents, marking a transgressive phase in the central Algarve sector. However, as with Facies D, assigning it unequivocally to a specific depositional setting remains challenging. The limited lateral continuity of the sandstones suggests a localized system. The presence of channelized geometries, trough cross-stratification, erosive bases, sigmoidal and flaser bedding, and upward-fining trends indicates channelized flow within a tidally influenced environment. Thus, Facies E may possibly represent tidal channels developed within a tidal flat setting (Daidu *et al.* 2013; Davis 2012; Hughes 2012). This interpretation is consistent with the stratigraphical transition from the underlying alluvial plain deposits (Facies A–C) and the heterolithic, tidalite-like, nature of the directly underlying Facies D. Nevertheless, the localized distribution, combined with the observed sedimentary structures and geometries of Facies E, is also compatible with a channels and tidal sand bars of the delta front facies (Davis 2012; Bayet-Goll & Neto de Carvalho 2016; Tinterii 2011; Goodbred and Saito 2012). The latter could have been potentially linked to a coastal pond setting, as a siliciclastic shelf environment appears less likely due to the absence of bioturbation, marine fauna, and lack of other associated unequivocally marine deposits. While the precise palaeoenvironmental interpretation remains uncertain, Facies E confirms the coastal character of the studied section.

Volcaniclastic and volcanic facies (Facies F)

Description.– Volcaniclastic and volcanic rocks have been observed only in the Vale do Álamo sections (Fig. 9A), overlying sandstones and red mudstones. Volcaniclastic sediments are represented by a discontinuous set of folded layers, up to 1 meter thick, of mudstone, fine ash and tuff, varying from black, grey, pale yellow, pale green, dark brown and red (Fig. 9B). Those layers are obliquely intersected by up to 1.5m thick undulating clast-supported layer consisting of basaltic, mostly brecciated, clasts supported by the finer volcanoclastic matrix (Fig. 9). Basaltic clasts range in size from dm- up to ca. 50 cm scale exhibiting globular, elongated, and angular shapes (Fig. 9C). In case of most observed clasts, their margins exhibit few centimetres thick yellow zones. This layer presents irregular, convoluted base, sinking into and deforming underlying fine-ash and tuffs (Fig. 9C). The sediments

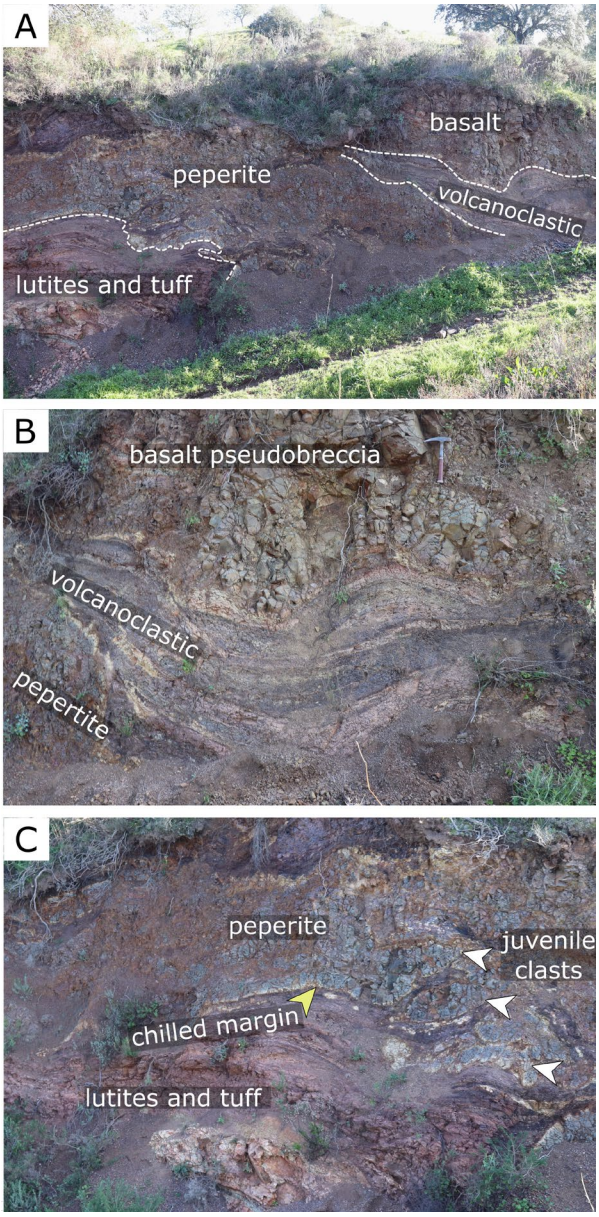

Fig. 9. Volcaniclastic and volcanic facies. A, exposure near the VA-1 section constitutes the top of the studied succession. Visible lateral transitions from fine-ash and tuff, peperite, volcanoclastic-rich layer and basalt. Note the irregular and convoluted boundaries between the layers, indicating significant sediment deformations. B, deformed, undulating volcanoclastic-rich layer with discernible black, grey, pale yellow, pale green, dark brown and red discontinuous layers and laminae covered by basaltic pseudobreccia. C, contact between prevalently red mudstones and tuffs and peperite composed of silt-sized volcanoclastic matrix and large brecciated basalt clasts. Note the yellow chilled margin at the lutite-tuff and peperite contact. Fluid-shaped basalt clasts with chilled margins occur near the contact with lutites and tuff.

mentioned are directly capped by a basaltic formation, which sits on an uneven surface formed by the contact between the volcaniclastic and basalt units. A distinctly undulating shape marks this interface. (Fig. 9A-B). The basalt layer represents the uppermost part of the examined sequence, forming a pseudobreccia that ranges in colour from dark grey to light green (Fig. 9B).

Interpretation.– Multiple volcanic and volcaniclastic successions have been recognized in and near the area of the Rocha da Pena (Lopes 2014; Martins *et al.* 2008; Pérez-López *et al.* 2021), which were suggested to represent an early-stage of CAMP volcanism (Pérez-López *et al.* 2021). Geochemical investigation of samples from localities close to Rocha da Pena indicated the subalkaline character of local volcanism (Martins *et al.* 2008; Pérez-López *et al.* 2021). Due to a lack of more detailed data, volcanoclastic layers are difficult to interpret, but they may refer to either pyroclastic fall, phreatomagmatic fall, or flow deposits (Martins *et al.* 2008). The clast-supported layer within the volcanoclastic succession presents features often observed in peperites, such as the presence of elongated and globular basaltic clasts (fluidal shapes suggesting the juvenile character of clasts) and glassy, yellowish outer margins suggesting rapid lava cooling upon contact with sediment and\or water (Carracedo *et al.* 2012; Chen *et al.* 2013; Martin & Nemeth 2007; Martins *et al.* 2008). The basaltic pseudobreccia is interpreted as a lava flow.

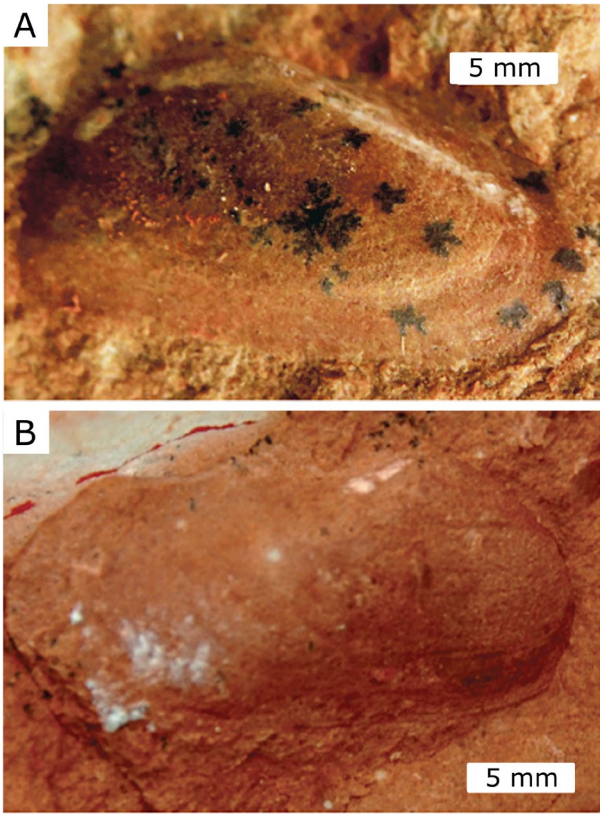

Fig. 10. Bivalve internal moulds. Field photos of moulds of Unionoida recovered near the *M. algarvensis* bonebed.

Faunal composition

Mudstone facies

Mudstone facies have been previously reported to yield remains of two temnospondyl amphibians: an indeterminate mastodonsaurid (Witzmann & Gassner 2008) and the metoposaurid *Metoposaurus algarvensis* (Brusatte *et al.* 2015). While mastodonsaurid remains are sparse, *M. algarvensis* fossils were recovered from a bonebed (Brusatte *et al.* 2015). Additionally, isolated phytosaur elements, including mandible and teeth, have been found near the bonebed (Mateus *et al.* 2014).

Here, we document the occurrence of bivalves from the RP1 section containing the *M. algarvensis* bonebed (Fig. 10). Their transversely elongated elliptical shells, umbo position, and moderate dorsal protrusion indicate an affinity with freshwater Unionidae (Bogan & Weaver 2012; Radley & Coram 2020; Skawina & Dzik 2011). Moreover, field prospection uncovered a layer of mudstone to calcareous mudstone (Fig. 11A) near the base of the VA 1 section, containing numerous isolated (Fig. 11B) and partially articulated actinopterygian fish scales (Fig. 11C).

Palustrine facies

Vertebrate remains are abundant in thin carbonate and calcareous mudstone beds associated with palustrine and calcrete facies. A hybodontid shark dorsal fin spine (Fig. 11D, E), identified by its subtle curvature, oval cross-section, distinct longitudinal groove, and ridge ornamentation (Carrillo-Briceño *et al.* 2016; Leuzinger *et al.* 2017; Maisey 1978; 1982; Zhang 2007), was recovered from palustrine calcareous mudstone. While already recorded in the Middle and Upper Triassic of Spain (Manzanares *et al.* 2017, 2018; Pla & Botella 2013), this specimen represents the first documented occurrence of hybodonts in the Triassic of Portugal.

Actinopterygian fish remains, common in palustrine facies, include at least four distinct ganoid scale morphotypes (Fig. 11F-I). Due to the isolation and relatively poor preservation of the material, coupled with the widespread occurrence of ganoid scales across various taxonomic groups (Cavin 2017; Helfman

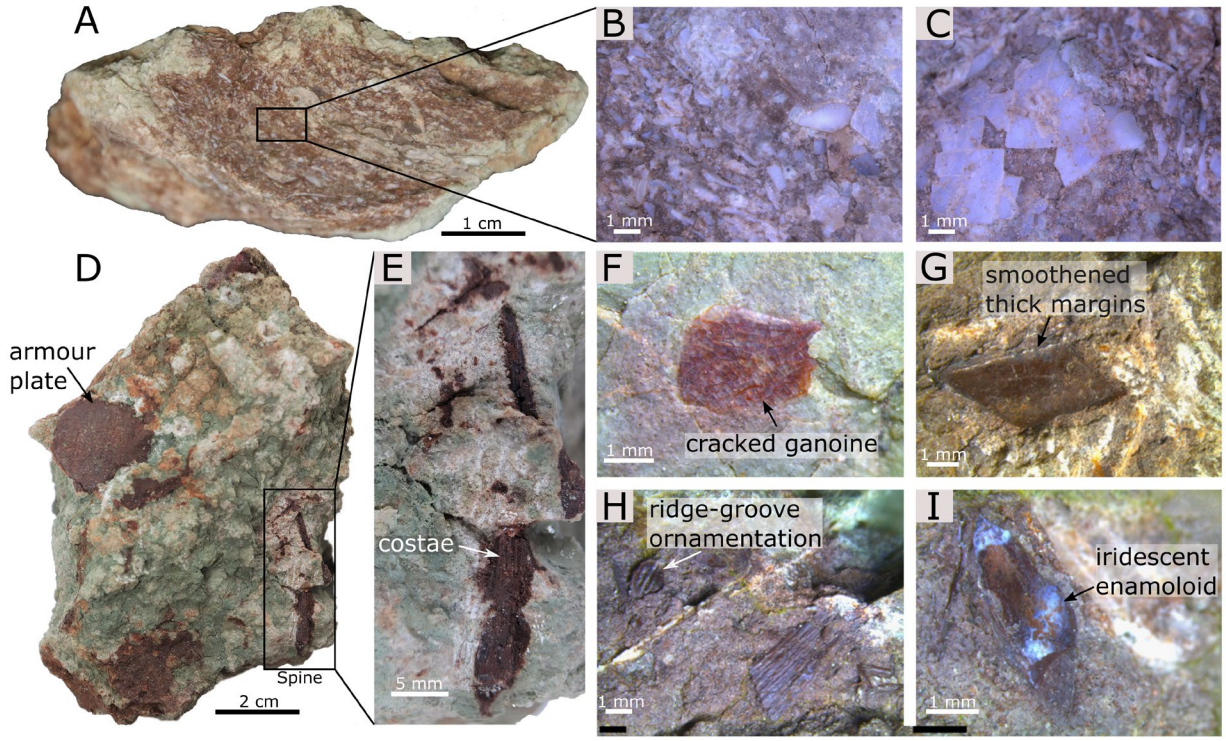

Fig. 11. Chondrichthyes and Actinopterygii remains from RP and VA outcrops. A-C, *Actinopterygii* scales uncovered from the scale-rich calcareous mudstone layer outcropping near VA - 1 section. A, calcareous mudstone block composed of numerous actinopterygian scales (white points). B, close-up of the part of the calcareous mudstone block exposing numerous, mostly fragmented scales. C, small group of articulated actinopterygian scales. D, E, calcareous mudstone block (from *Henodus* layer) containing a placodont armour plate and a hybodontid fin spine (FCT-UNL 620). E, hybodontid fin spine. F-I, Actinopterygian scale morphotypes recovered from the *Henodus* layer. F, morphotype one. G, morphotype two. H, morphotype three. I, morphotype four.

et al. 2009), precise identification is hindered. Thus, all morphotypes are assigned to Actinopterygii indet. However, tentative taxonomic affinities can be discussed. Rhomboidal to nearly rectangular ganoid scales with 'peg and socket' articulation (Fig. 11F) resemble those of Ginglymoid, particularly Semionotiformes (Antczak & Bodzioch 2018; Heckert, 2004; Kowalski *et al.* 2019; Kovalchuk & Anfimova 2020). Elongated, rhomboidal, thick ganoid scales (Fig. 11G), while also found in Semionotiformes, are frequently attributed to Redfieldiidae (Heckert 2004; Heckert *et al.* 2012; Khalloufi & Jalil 2020; Kim *et al.* 2020 and references therein). Scales with distinct groove and ridge ornamentation (Fig. 11H) are comparable to those of Palaeoniscidae (Heckert 2004; Mears *et al.* 2016; Pawlak *et al.* 2022; Ronan *et al.* 2020). However, we emphasise that more complete or diagnostic actinopterygian material is necessary for an accurate taxonomic identification.

Tetrapod remains from palustrine facies include isolated armour plates (Fig. 12A-C), ribs (Fig. 12D), long bone fragments (Fig. 12E) and vertebrae (Fig. 12F). Rib, long bone and vertebral material exhibit features consistent with henodontid placodonts. However, their precise taxonomic identification remains uncertain (see Supplementary Materials). Moreover, the skull fragment has been attributed to *Henodus* sp., while the armour plates, though possibly originating from the same taxon, exhibit features characteristic of cyamodontoid placodonts (Ruciński *et al.* 2025). Placodont remains, including similar armour plates, were previously recorded in Iberia from the Upper Triassic of Spain (de Miguel Chaves *et al.* 2020).

Morphological descriptions and details of taxonomic identifications of the presented fossil material are provided in the Supplementary Material.

Taphonomic observations

Field observations of palustrine beds

Description.– Most collected specimens from palustrine carbonates and calcareous mudstone beds are isolated, fragmentary, and poorly preserved (Fig. 12). Complete specimens, primarily armour plates, are rare. The latter exhibit various stages of preservation (Fig. 12A-C), with most specimens exhibiting distinct

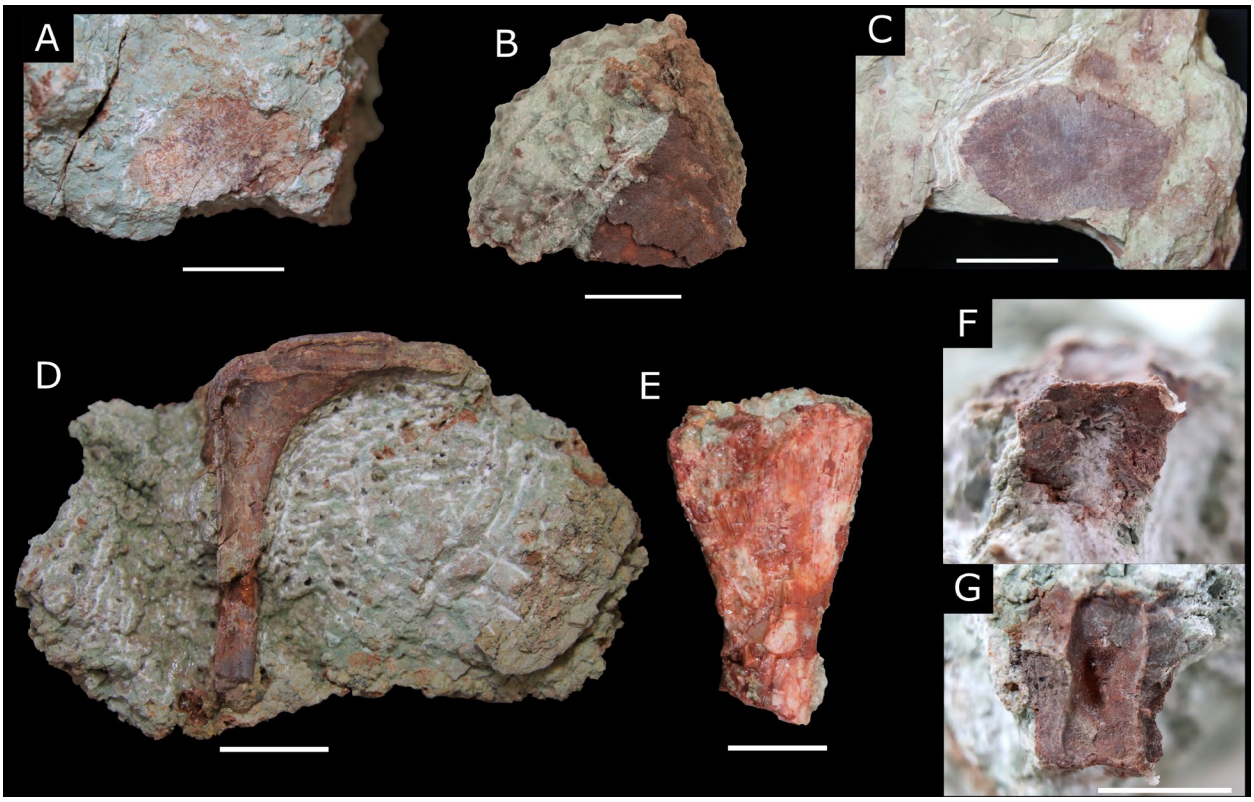

Fig. 12. Reptile remains showing possible affinities to *Henodus*. A-C, placodont armour plates exhibiting various stages of preservation. A, oval-shaped armour plate (FCT-UNL 629) from palustrine limestone characterized by a weathered, cracked surface and eroded margins. B, armour plate (FCT-UNL 625) from calcareous mudstone (*Henodus* layer) characterized by a distinct degree of weathering (flaking out of bone surface) and fragmentation. C, elongated armour plate (FCT-UNL 630) from palustrine limestone resembling plates from the central portion of *Henodus* carapace (Reiff 1937; Westphal 1976). The specimen shows comparatively good preservation with limited fragmentation and weathering restricted to bone surface cracking. D, fragment of holocephalous ribs characterized by an expanded, trapezoidal capitulum (FCT-UNL 631). Element exhibits moderate surface cracking and red staining. E, fragment of an unidentified limb element (FCT-UNL 632), displaying a distinct degree of surface alteration and red staining. Vertebral centrum (FCT-UNL 626) displaying a high degree of weathering alterations in F, caudal and G, dorsal view. Scale bars equal 1 cm.

weathering and altered margins. Ribs and long bones are represented either by rib or long bone heads with incomplete portions or only parts of the shaft (Fig. 12D, E). Vertebral centra (Fig. 12F, G), albeit relatively complete, show signs of distinct weathering and lack neural arches. Small-sized, unidentifiable bone flakes are the most commonly found remains, occurring abundantly both in isolated blocks and as finds in situ of excavated beds. Actinopterygian scales are, in most cases, represented by isolated specimens, often fragmentary.

All bones obtained from isolated blocks and directly from the layers investigated are characterized by dark red to brown colouration. All gathered specimens exhibit signs of weathering, although of highly variable degree, bracketing stages 1-3 of Behrensmeyer's (1978) scale. However, most specimens exhibit distinct cracking and flaking of the outermost bone layer (stage 2), sometimes reaching the trabecular bone (stage 3).

Interpretation.– A significant degree of fragmentation, the occurrence of only isolated remains, and close co-occurrence of fossils belonging to different taxa in small accumulations suggest distinct dissociation and some rate of the redeposition of those skeletal elements (Rogers *et al.* 2007). However, the exact transportation rate of those remains cannot be attested based on observations gathered so far.

Different stages of preservation and weathering suggest variable degrees of skeletal element exposure to aerial conditions. However, the prevalence of advanced alterations signifies the prolonged exposure of most studied skeletal elements (Behrensmeyer 1978; Fernandez-Jalvo & Andrews 2016). That can be further supported by many bone flakes in the studied beds, suggesting that a large portion of skeletal material has been partially disintegrated before burial. Red staining signifies a high rate of bone Fe permineralization (Bao *et al.* 1998; Fernandez-Jalvo & Andrews 2016).

The fossil-bearing calcareous mudstone and palustrine beds have been affected by pedogenesis, which likely contributed to the overall poor preservation of the specimens through early diagenetic alteration. Weathering during recent exhumation may have further degraded specimens in isolated blocks; however, even skeletal elements recovered directly from the layers, thus not exposed to recent weathering, show similar preservation. Therefore, the alteration of animal remains can be primarily attributed to processes occurring before (weathering) or shortly after burial (early diagenesis).

The lack of invertebrate remains is conspicuous, considering common vertebrate fossils in palustrine facies. The factors behind this observation are not yet clear. However, they are likely related to sampling bias and/or diagenetic processes, which may lead to the dissolution and depletion of aragonitic invertebrate material.

Late Triassic mollusc faunas from the marginal to marine environments are often recorded to be of small sizes, not exceeding a few millimetres in diameter (Goy & Aliaga 1998; Hausmann *et al*. 2021; Santos *et al*. 2022). This is also the case for the studied samples from the Ayamonte area, located in the easternmost part of the Algarve Basin (Santos *et al*. 2022). Thus, they could be overlooked without the application of specific methods that aim at obtaining the microfossils.

Alternatively, owing to the observed strong influence of pedogenetic processes on the fossiliferous beds showing signs of neomorphism, calcium carbonate shells were likely to be dissolved and not preserved in highly re-cemented beds. Moreover, the early diagenetic processes are thought to be responsible for a significant depletion of aragonite shell material due to its dissolution, especially in low-energy and/or high-organic-content environmental settings (Cherns *et al*. 2010; Cherns & Wright 2009; Sulpis *et al*. 2022).

Histotaphonomic observations

Description.– During the study, a thin-section of palustrine packstone containing a fragment of placodont armour plate was analysed (Fig. 13). Armour plate is characterized by a relatively low degree of vascularization (Scheyer 2007) (Fig. 13A). Bone tissues are phosphatic, while the vascular pores are filled with microspar and occasionally with iron oxide. (Fig. 13B). In some observed vascular pores, the red iron oxide coating occurs as a thin rim stretching along the bone margin. The bone plate exhibits multiple, mostly oblique fractures filled with iron oxides (Fig. 13C). However, wider, unfilled fractures extend throughout the sediment and bone. In this section, the boundaries of the bone plate are largely irregular, with common incisions cutting into the bone (Fig. 13C). Locally at the bone-sediment contact, the small iron-oxide film stretches (Fig. 13D). In proximity to the bone plate, local accumulations of lumpy peloids occur (Fig. 13D).

Interpretation.– The large degree of bone surface alteration, characterized by irregular margins, indicates partial dissolution of bone. Frequent fractures filled with iron oxides and locally occurring red iron-oxide film at the bone margin indicate intensive Fe-permineralization of the bone, concurrent with red staining of the bone surface. Fe permineralization is found to be common in pedogenetically affected settings due to high iron availability in ferromagnesian mineral-rich sediments and its mobility induced by oscillating groundwater levels and changes in redox conditions (Bao *et al*. 1998; Mancuso & Previtera 2022). In periods of high groundwater level, iron hydroxide could form under reducing conditions in aqueous solutions and subsequently be transformed into hematite (Fe_2O_3) or goethite (FeOOH) under oxic conditions, which are pervasive at times of low water level (Mancuso & Previtera 2022). At the early stage of diagenesis, iron-rich fluids can percolate into buried bones through multiple fractures, likely linked to a distinct degree of weathering, and form iron oxides inside the voids.

Microspar filling the bone canals implies the infiltration of calcium-carbonate-rich fluids into a bone (Kowal-Linka 2015). There are two main explanations concerning microspar formation. Traditionally, microspar formation was attributed to aggrading neomorphism (recrystallization), often linked to meteoric diagenesis and subaerial exposure (Flügel & Munnecke 2010). This would be consistent with the palustrine depositional setting of the studied beds. However, microspar forming as a primary cement at an early stage of diagenesis, including one-step neomorphic recementation of aragonite mud into calcitic microspar crystals, has also been postulated (Flügel & Munnecke 2010; Munnecke *et al.* 1997).

The analysed sample displays at least two permineralization events: early iron oxide precipitation in vascular canals and fractures, followed by microspar formation (either as primary cement or via re-cementation). Some iron oxide may have also formed during later diagenetic stages, filling wider fractures without microspar, suggesting specimen exhumation (Mancuso *et al.* 2017). These observations align with diagenetic patterns seen in vertebrate fossils from alluvial plains of semi-arid to arid climates (Mancuso & Previtera 2022).

Clusters of lumped peloids surrounding the bone are conspicuous, as they are otherwise scarce in the thin section. While their occurrence cannot be

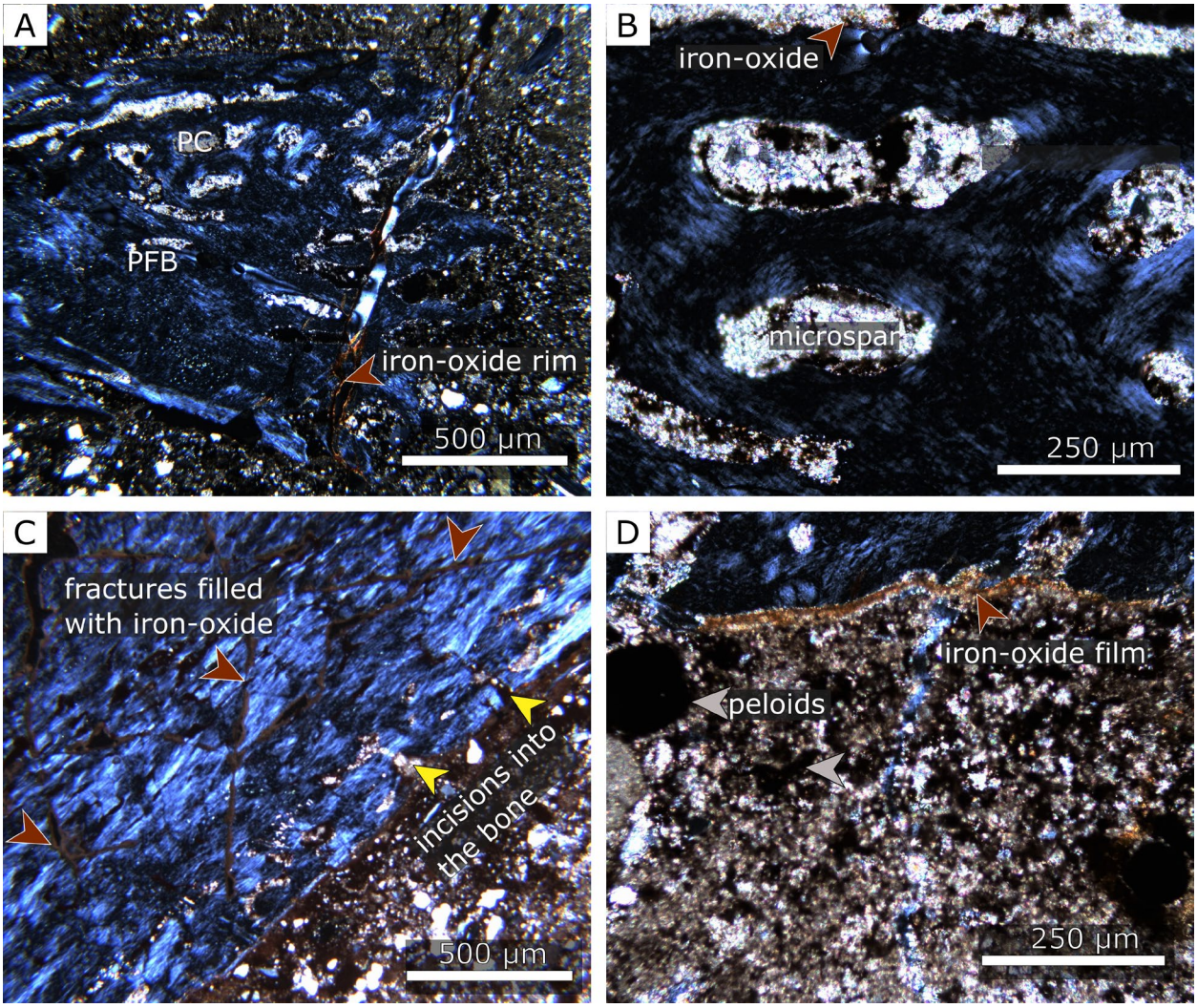

Fig. 13. Microphotographs of palustrine carbonate sample containing placodont armour plate. A, bone histology of placodont armour plate. Primary canals (PC - example indicated by red arrow) are filled with microspar. Note the largely irregular margins of the plate and large crack, indicating a significant pedogenesis/diagenetic alteration. B, close-up of the primary canals filled with microspar and surrounding primary parallel-fibred bone. C, close-up of the armour plate exhibiting numerous fractures filled with iron oxide (indicated by red arrow) and breakages at the bone margin (yellow arrow). D, close up on the bottom margin of the bone plate and surrounding sediment rich in clumps of large peloids. Note the thin, red iron-oxide film at the bone-sediment contact (indicated by the red arrow).

uncontestably explained, they may be linked to microbiolitic activity associated with decaying organic matter (Danise *et al.* 2012; Shapiro & Spangler 2009).

Discussion

Palaeoenvironmental conditions during the deposition of fossiliferous layers

The fossiliferous beds in the Rocha da Pena were formed in a continental mudflat system dominated by frequent drainage and/or water table oscillations (Fig. 14). The observed depositional processes vary from subaerial and arid conditions to palustrine and humid periods (Fig. 14A). The heterolitic and repetitive character of the studied succession points to a possible climatic control on its deposition (Bahr *et al.* 2020; Jewuła *et al.* 2019; Jewuła *et al.* 2023; Reinhardt & Ricken 2000; Vollmer *et al.* 2008). Additionally, the site's location within a tectonically active rift basin, evidenced by common syn-sedimentary faults, suggests that basin subsidence and/or tectonic activity affecting accommodation and sediment input might have played a role in modulating depositional patterns (Breda & Preto 2011; Huerta *et al.* 2011; Jewuła *et al.* 2023; Leleu *et al.* 2016; Ortí *et al.* 2017; Platt & Wright 2023).

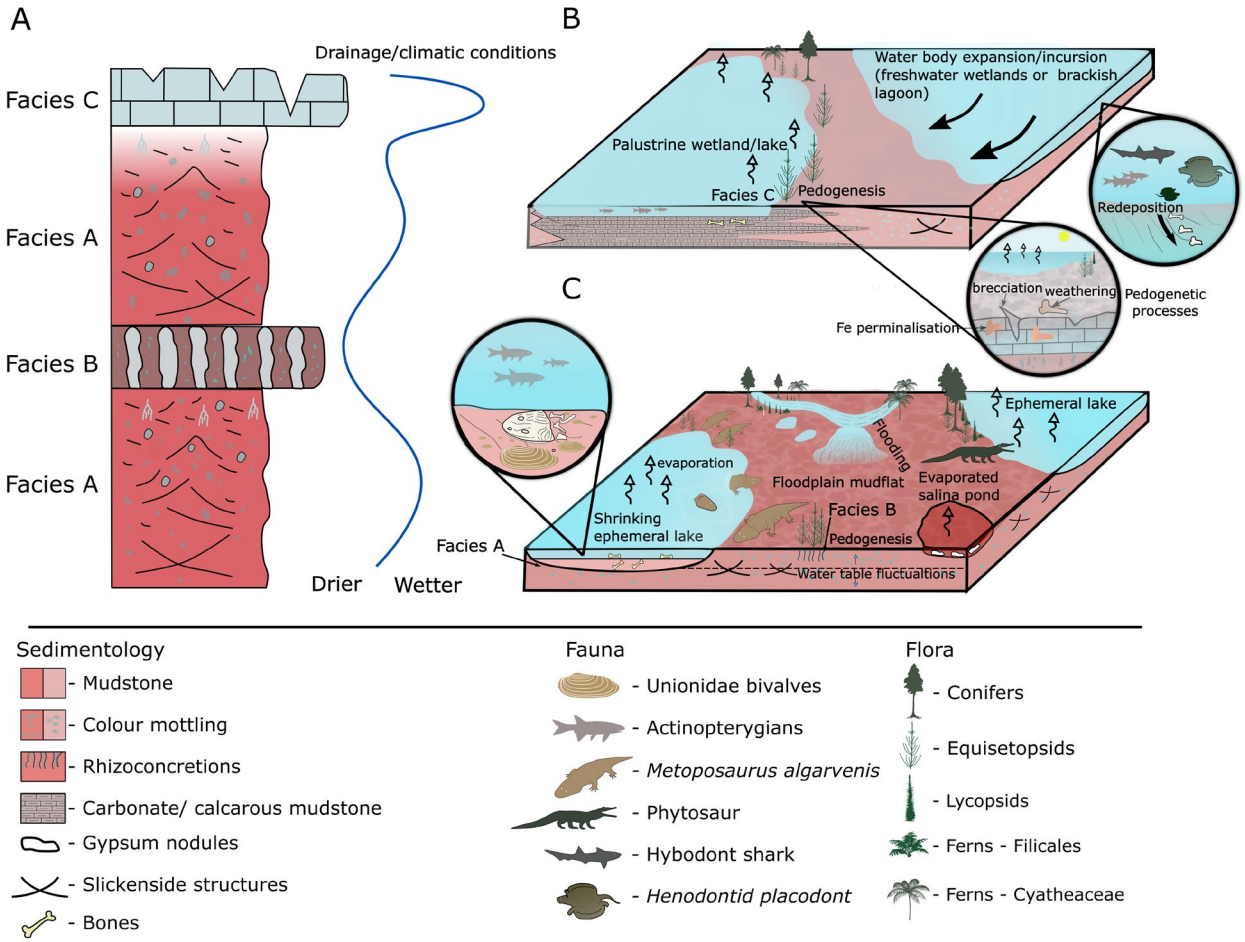

Fig. 14. Schematic reconstruction illustrating the depositional model for the Upper Triassic Rocha da Pena deposits of the Algarve Basin. A, schematic depositional model illustrating mudstone, calcrete and palustrine facies relationship and their connection to drainage and/or climatic conditions. B, C, palaeoenvironmental reconstruction of the studied area with illustrated associated fauna. B, palustrine setting is constructed to represent, at least locally, more humid conditions and deposition within shallow lake\wetlands. The potential impact of marine incursions on the deposition of these facies is considered a possible, but not yet confirmed, scenario. Remains of aquatic taxa were disassociated, likely due to hydrodynamic processes, and subsequently altered by subaerial exposure and pedogenic processes. C, playa floodplain and lakes\ponds with deposition of mudstone and calcrete facies and freshwater fauna. The concentrated abundance of aquatic faunal remains, especially *Metoposaurus,* is hypothesized to be linked with biogenic aggregation. The disassociation of elements is consistent with flooding observed in alluvial mudflat settings.

During the Late Triassic, the climate was characterized by hot-house conditions and predominantly non- or poorly developed zonal patterns (Preto *et al.* 2010; Sellwood & Valdes 2006), with possible regional and temporal changes in climatic zonation (Tanner 2018). Nonetheless, monsoonal circulation largely influenced the climatic conditions, dependent on the proximity to the Tethys or Panthalassa oceans (Parrish 1993; Preto *et al.* 2010; Tanner 2018).

Although the exact position of Iberia during the Late Triassic is challenging to establish (Terrinha *et al.* 2019 and references therein), this area corresponded to the low latitude in the approximate range of 10°- 20°, possibly up to 30° N (Golonka 2007; Ortí *et al.* 2017; Scotese & Schettino 2017; van Hinsbergen *et al.* 2015). At that time, the Algarve Basin was located on the southern Laurasian margin near the western branch of the Neotethys, formed in the Maghrebian-Gibraltar rift (Arche & López-Gómez 2014; Azerêdo *et al.* 2003; Ortí *et al.* 2017). Transient marine influences are indicated by Triassic mudrock minerals such as smectite, sepiolite and corrensite (Trindade *et al.* 2010). Proximity to the Neotethys is also evidenced by palynological records of freshwater/brackish algae (i.e. *Botryococcus* sp., *Ovoidites* sp., *Plaesiodictyon mosellanum* ssp. *bullatum* and *Plaesiodictyon mosellanum* ssp. *variable*) found throughout the Silves Marl-Carbonate Evaporitic Complex (Vilas-Boas *et al.* 2024). The identification

of tidal or deltaic deposits in the VA2 section, attributed to the upper part of the Silves Marl-Carbonate Evaporitic Complex, further corroborates the marine influence in the studied area. Consequently, the region likely experienced a semi-arid, seasonal, monsoonal climate (Parrish 1993; Preto *et al.* 2010).

Such climatic conditions could have been well represented by the alternation between variegated but prevalently red mudstones and carbonate levels in the studied area. The semi-arid and highly seasonal conditions inferred from mudstones with common pedogenetic features, including the formation of calcretes and evaporites, are corroborated with commonly occurring xerophytic flora indicated by previously recorded pollens (e.g. *Alisporites* sp., *Camerosporites secatus*, *Ellipsovelatisporites* sp., *Enzonalasporites vigens*, *Microcachrydites* spp., *Patinasporites densus*, *Vallasporites ignacii*) within the Silves Marl-Carbonate Evaporitic Complex (Vilas-Boas 2023; Vilas-Boas *et al.* 2024). Moreover, these observations are consistent with the geochemical analysis of the Triassic mudstones in the Algarve region, which reveals high contents of magnesium, dolomite, hematite, and illite (Trindade *et al.* 2010).

Although environmental fluctuations in the depositional setting have been recognized, it was predominantly a low-energy system. Most of the succession consists of mudstones with intercalated palustrine carbonates, both exhibiting pedogenetic features. This indicates deposition within an alluvial plain setting (Fig. 14C, D) under a seasonal and semi-arid climate, which can be characterized as a playa mudflat system with recurring palustrine conditions (Archer *et al.* 2022; Bahr *et al.* 2020; Jewuła *et al.* 2019; Jewuła *et al.* 2023; Szulc *et al.* 2015; Vollmer *et al.* 2008). Analogous coeval records of ancient alluvial plain and palustrine settings are known, for example, from the Germanic Basin (i.e., Germany, Poland) and Chinle Formation (USA) related to the succession of Triassic humid and arid episodes (Bahr *et al.* 2020; Jewuła *et al.* 2019; Reinhardt & Ricken 2000; Szulc *et al.* 2015; Tanner & Lucas 2006; Vollmer *et al.* 2008).

In such a setting, the mudflat surface would be seasonally flooded during the wet season, resulting in the formation of ephemeral lakes and ponds, in which mud would deposit from suspension or during the waning energy of the water flow (Jewuła *et al.* 2019; Milroy *et al.* 2019; Smith 2003). During drier periods, water bodies shrank or evaporated, exposing sediments to aerial conditions and pedogenetic processes. Longer aerial exposure and/or changes in drainage conditions led to the development of some of the mudstone beds into calcretes (Alonso-Zarza & Wright 2010; Wright & Tucker 2009). Locally, the studied area was temporarily covered by vegetation, as suggested by layers containing numerous rhizoconcretions (Kraus & Hasiotis 2006). Red beds containing the accumulation of large gypsum nodules suggest episodes of drier climate and increased evaporation, leading to the formation of salina ponds/lakes and/or an increase of the sulphate fraction in groundwaters, leading to the precipitation of gypsum (Bustillo *et al.* 2017; Eckardt *et al.* 2001; Huerta *et al.* 2010). The absence of horizon A indicates a truncated palaeosol due to erosion (e.g. Kraus 1999; Tabor & Meyers 2015). The alternation of very weak Bw and Bwk horizons, or even K, suggests a composite profile related to sporadic deposition, probably less than 2 km from a water channel (Marriott & Wright 1993; Kraus 1999). These zones are characterized by rapid floods with long recurrence periods, enhanced soil development, and poor overlap with the younger horizons (e.g. Kraus & Alsan 1995; Kraus 1999).

During episodes of larger water supply, the palustrine carbonates were formed in either peripheral lacustrine, wetland or lagoonal environments (Alonso-Zarza 2003; MacNeil & Jones 2006; Platt & Wright 1992; Platt & Wright 2023). Nevertheless, the formation of the carbonate beds must have occurred in relatively shallow water bodies with low-gradient settings. The calcium carbonate would precipitate within the water bodies, likely induced or enhanced by microbial activity, followed by the water evaporation and subaerial to aerial sediment exposure (Alonso-Zarza 2003). Changes in topography leading to differentiation of extension and aerial exposure of palustrine beds might have also contributed to the observed textural variability (Marty & Meyer 2006; Huerta *et al.* 2011; Jewuła *et al.* 2023; Platt & Wright 2023).

Based on the provided observations and recent palynological data (Vilas-Boas *et al.* 2024), the mudstone-carbonate facies at Rocha da Pena likely represents a paralic environment. This setting consisted of a coastal floodplain, with episodically forming or expanding palustrine lakes or wetlands, yet to a fully defined degree of marine influence. This interpretation is consistent with findings from the Upper Triassic Ayamonte sector, which records transitions from coastal alluvial plains to brackish lagoons and shallow marine environments (Santos *et al.* 2022). However, the Ayamonte sector exhibits a stronger marine signal than Rocha da Pena, possibly due to its closer proximity to the Neotethys branch.

While a precise comparison and correlation with other Iberian stratigraphical sequences lies beyond the scope of this paper, we observe notable similarities between the depositional sequences of the

Algarve Basin and those of the Keuper succession (K1-K5 units) in southern and eastern Iberia (López-Gómez *et al*. 2019; Ortí *et al*. 2017; Pérez-López 1996; Suárez 2007). The studied Penina section is particularly reminiscent of the middle Keuper facies, especially unit K3 of the Prebetic-Subbetic and Iberian Basins in Spain, which has been interpreted as representing a saline mudflat environment within a coastal plain setting subjected to occasional marine conditions (Pérez-López 1996; Suárez 2007). This interval is characterized by thick units of predominantly red, locally variegated claystones and siltstones, containing dispersed gypsum nodules and relatively thin intercalations of carbonate, calcrete, and sandstone (Pérez-López 1996), thus comparable to the facies associations presented in this study.

As in the Algarve Basin, in the Spanish succession these deposits are preceded by fluvial sandstones of the K2 unit (Silves Sandstones in the Algarve) and followed by thick evaporitic deposits of K4–K5 units (thick evaporite beds of the uppermost part of the Silves Marl-Carbonate Evaporitic Complex in the southern sector of the Algarve) (Arche *et al*. 2014; López-Gómez *et al*. 2019; Ortí *et al*. 2017; Pérez-López 1996; Suárez 2007). Furthermore, the thicker carbonate-rich succession of the Zamoranos Formation parallels the carbonate units recorded in the Ayamonte sector of the Algarve Basin (Santos *et al*. 2022; Pérez-López *et al*. 2012)

Although we do not propose direct stratigraphical equivalence between these units, acknowledging that the facies may be diachronous due to regional variations in basin accommodation and proximity to the Tethys margin, the overall depositional architecture suggests a comparable sedimentary evolution across both regions. This study of the central sector of the Algarve Basin supports the interpretation that the area represents a coastal environment, constituting the westward continuation of the coastal facies of the South Iberian palaeomargin identified in southern Spain. Nonetheless, we emphasize the need for geographically broader comparative studies that account for spatial facies stacking patterns within the Algarve Basin before detailed stratigraphical correlations with the Spanish successions can be established robustly.

Faunal assemblage and taphonomy of the mudstone beds

The ephemeral/lacustrine water bodies formed within the mudflat system would have provided the habitat for freshwater unionoid bivalves, actinopterygians and aquatic tetrapods such as metoposaurs and phytosaurs (Fig. 14C). Those taxa constitute common components of the Late Triassic assemblages recovered from lacustrine and floodplain deposits (e.g. Bodzioch & Kowal-Linka 2012; Buffa *et al*. 2019; Dzik & Sulej 2007; Lucas *et al*. 2010; Milner & Schoch 2004; Moreno *et al*. 2024; Rakshit & Ray 2021). However, the detailed taphonomy of the *Metoposaurus* bonebed (Brusatte *et al*. 2015) has yet to be elaborated.

Based on the material recovered to date, the Rocha da Pena bonebed constitutes a monodominant assemblage with numerous *Metoposaurus algarvensis* remains (Brusatte *et al*. 2015), accompanied by sparse actinopterygian scales. The monodominant nature and exclusive presence of aquatic taxa suggest a biogenic aggregation origin of this assemblage (Lucas *et al*. 2010; Kufner *et al*. 2025). The common occurrence of evaporites within mudstone facies, particularly of large gypsum nodules near the bonebed, indicates fluctuating, arid climatic conditions marked by ephemeral water bodies subject to rapid evaporation. Such conditions could have contributed to mass mortality among aquatic fauna (Brinkman *et al*. 2007; Godfree *et al*. 2019; Haag & Warren 2008; Lucas *et al*. 2010; Matthews & Marsh-Matthews 2003). Within this palaeoenvironmental framework, mass mortality due to desiccation of aquatic habitats remains a plausible explanation for the initial accumulation of *Metoposaurus* remains. However, alternative scenarios, such as behavioural grouping patterns, eutrophication or flood-induced mortality, cannot be ruled out at this stage (Bodzioch & Kowal-Linka 2012; Kufner *et al*. 2025; Rakshit & Ray 2021).

Distinct fossil disarticulation and common fragmentation (see figures in Brusatte *et al*. 2015) suggest dissociation and a possible, but yet unknown degree of re-deposition, consistent with an alluvial plain setting where flood events may disarticulate animal remains, as observed in metoposaurid-bearing sites like Lamy Quarry (Lucas *et al*. 2010) Rotten Hill (Lucas *et al*. 2016); Nobby Knob (Kufner *et al*. 2025); Tiki bonebeds (Rakshit & Ray 2021), and Krasiejów (Bodzioch & Kowal-Linka 2012; Szulc *et al*. 2015). Unlike the multitaxic Rotten Hill, taxonomically diverse Krasiejów, and Tiki bonebeds, the monodominant Rocha da Pena bonebed shows a stronger resemblance to the Lamy Quarry and Nobby Knob localities, which consist mostly of disassociated metoposaurid remains (Kufner *et al*. 2025; Lucas *et al*. 2010). In both instances, the accumulation of skeletal elements within a floodplain setting is interpreted as evidence of biogenic aggregation. However, the degree of subsequent redeposition of animal remains differs between the sites, being more pronounced,

but still relatively limited, in the Lamy Quarry (Lucas *et al*. 2010; Kufner *et al*. 2025).

At present, we lack detailed data on skeletal element sorting, which could elucidate the origin of the Rocha da Pena bonebed. However, the presented observations allow us to formulate a preliminary hypothesis that the Rocha da Pena bonebed resulted from biogenic, possibly drought-induced aggregation, followed by disassociation and an unknown degree of re-deposition of skeletal elements in a floodplain setting. Due to a lack of more robust and detailed taphonomical data, we emphasize that further studies of the Rocha da Pena *Metoposaurus* bonebed are required to confirm the preliminary hypothesis.

Faunal and taphonomy of the palustrine beds – possible facies-based faunal differentiation

Palustrine carbonates and mudstone facies exhibit distinct faunal assemblages. While mudstone beds contain freshwater fauna, initial prospection of palustrine facies reveals predominantly placodont and actinopterygian remains (Fig. 14B). Apart from similar actinopterygian scale morphotypes, no shared taxa have been identified in both facies. Given the early stage of palustrine bed exploration, the current faunal record may be undersampled, introducing potential bias. However, the relative abundance of placodont remains (primarily armour plate fragments) in carbonate beds, in contrast to their absence in well-studied mudstone layers, supports the differentiation of faunal assemblages. Therefore, distinct palaeoenvironmental conditions and/or different taphonomic processes influencing skeletal accumulation should also be considered.

Based on the sedimentological and palaeontological evidence, three scenarios of the faunal remain accumulation in palustrine beds are here considered: 1) fauna predominantly represented by actinopterygians and placodonts, adapted to the freshwater environment was accumulated in freshwater bodies within shallow lacustrine/palustrine setting; 2) palustrine to shallow lacustrine setting characterized by elevated salinity compared to ephemeral freshwater water bodies recorded in mudstone facies; and (3) placodont dominated assemblage derived from marine\brackish environment during inland water incursion.

In the first scenario, faunal differences may stem from sampling bias or environmental shifts, such as the formation of perennial water bodies, which might have been more suitable for placodonts. However, the absence of typical freshwater taxa, like those recorded in mudstone facies, would remain conspicuous. The second scenario suggests that salinity variations exist, with freshwater fauna in mudstone beds and more saline conditions in palustrine facies. This could explain the prevalence of placodont remains and the absence of typical freshwater species. The third scenario posits a direct marine influence, comparable to the Upper Triassic Travessa Formation in Italy, where lagoonal flooding recurrently interrupted continental floodplain sedimentation (Breda & Preto 2011). Comparable fluctuating marine influences have been proposed for the Ayamonte sector of the Algarve Basin (Santos *et al*. 2022) and the Prebetic-Subbetic Basins in Spain (Pérez-López 1996).

Palynological analysis suggesting the presence of brackish waters (Vilas-Boas *et al*. 2024), proximity to the Neotethys (Santos *et al*. 2022), and so far coastal\lagoonal records of henodontid placodonts (García-Ávila *et al*. 2021; Pommery *et al*. 2021) suggest that salinity fluctuations and punctuated marine influence can be considered as a possible factor behind faunal assemblage differentiation in the studied beds. However, due to the lack of characteristic brackish\marine invertebrate fauna in palustrine beds, this hypothesis cannot yet be proved for the Rocha da Pena site.

Undoubtedly, the final accumulation of animal remains from palustrine facies occurred in a continental setting, with skeletal elements subjected to a distinct degree of dissociation and likely redeposition. Subsequently, the vertebrate remains were distinctly altered due to subaerial exposure of the palustrine beds and the action of pedogenetic processes, leading to a marked degree of weathering and Fe permineralization of skeletal elements. Moreover, these same processes and the re-cementation of carbonate beds may have contributed to the depletion of invertebrate shell fossil material. We emphasize that more extended fossil sampling and palustrine carbonate study are required to constrain palaeoenvironmental conditions and confirm the observed faunal disparity between the mudstone and palustrine facies.

Stratigraphical and temporal framework of the Rocha da Pena Site

Based on the lithological and sedimentological properties, the mudstone-carbonate deposits are assigned to the Silves Marl-Carbonate Evaporitic Complex (Fig. 15). The location of the fossiliferous levels 3 m below the silty-sandstone deposits and 10 m below volcanic rocks representing the upper to the uppermost part of the Silves Group, confirms the position of fossiliferous beds within the upper portion of the Silves Marl-Carbonate Evaporitic Complex (Fig. 15).

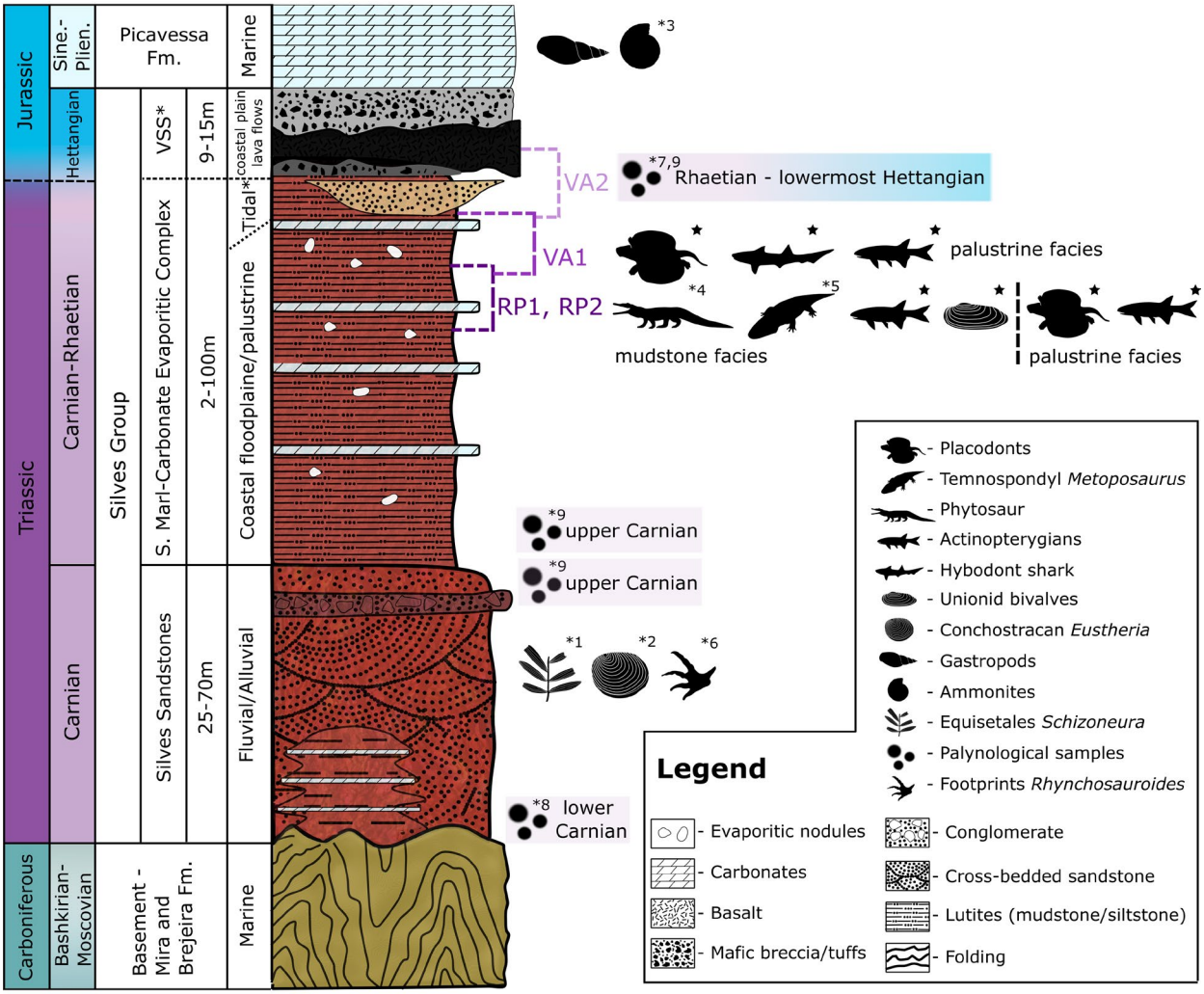

Fig. 15. Schematic stratigraphical log of the Silves Group exposed in the central area of the Algarve Basin summarizing palaeoenvironmental and palaeontological data. Numbers associated with animal and plant silhouettes refer to primary references stating their occurrence: 1 - Teixeira 1948; 2 - Palain 1976; 3 - Rocha 1976; 4 - Mateus *et al.* 2014; 5 - Brusatte *et al.* 2015; 6 - Mayoral *et al.* 2016; 7 - Pérez-López *et al.* 2021; 8 - Vilas-Boas *et al.* 2022; 9 – Vilas Boas *et al.* 2024; Star - this study. Based on published palynological records, chronostratigraphical constraints are indicated alongside the palynological samples presented in the log. Gastropod and bivalve (Santos *et al.* 2022) and sauropterygian (Reolid *et al.* 2022) records are also described from the Ayamonte sector in the westernmost part of the AB. VSS – Volcano-Sedimentary Series; Fm. – Formation.

The Silves Marl-Carbonate Evaporitic Complex has been recently constrained using palynological records to range between the upper Carnian and the upper Rhaetian–lowermost Hettangian (Vilas-Boas *et al.* 2024). The mudstone-carbonate unit from Rocha da Pena has been analysed in terms of pollen and algae content; however, in this, as well as the Vilas-Boas study (Vilas-Boas 2023) no palynological records have been recovered. Thus, the vertebrate fossils are currently the only source of biostratigraphical information for mudstone-carbonate succession in Rocha da Pena.

The presence of Julian Henodontidae (García-Ávila *et al.* 2021), Julian to Lacian/Alunian *Metoposaurus* (Buffa *et al.* 2019; Lucas 2020; Moreno *et al.* 2024), and phytosaur remains exhibiting plesiomorphic characters (Mateus *et al.* 2014), recently assigned to Tuvalian to Lacian *Angistorhinus* cf. *talainti* (López-Rojas *et al.* 2025), suggests an older age, mostly consistent with Carnian, and to a lesser extent, Norian, within the constrained upper Carnian to uppermost Rhaetian/lowermost Hettangian interval. However, the sparse record of Henodontidae (de Miguel Chaves *et al.* 2018; von Huene 1936; 1938) and the broad stratigraphical ranges of *Metoposaurus* (Buffa *et al.* 2019; Lucas 2020; Moreno *et al.* 2024) render these taxa poor biostratigraphical markers. Phytosaur genera are typically more temporarily constrained, providing

higher biostratigraphic resolution; however, in the absence of independent age constraints, age determinations based solely on phytosaur remains should be interpreted cautiously (Stocker & Butler 2013; Stocker *et al.* 2017; Butler *et al.* 2019; Brownstein 2023; Datta & Ray 2023). Thus, a younger age for the Rocha da Pena fossil-bearing deposits, which could be provisionally suggested by its position in the upper portion of the Silves Marl-Carbonate Evaporitic Complex, cannot currently be excluded. Consequently, further studies are necessary for more precise dating of the vertebrate-bearing strata within the Silves Group.

Attributing the silty and sandstone sediments of the Facies E to the specific unit is problematic, as those deposits have not been precisely described and referred to in any published works. In the unpublished thesis, Lopes (2006) assigned those sediments to *Complexo Vulcano-Sedimentar* sensu Manupella (1992). However, we did not observe volcanic or volcanoclastic layers interbedded with siltstone and silty-sandstone facies, which are noted to overlie the sandstones of Facies E. Consequently, as the overlying volcanic and volcanoclastic deposits can be firmly attributed to the Volcano-Sedimentary Series, the silty and sandstones of Facies E are tentatively attributed to the uppermost part of the Silves Marl-Carbonate Evaporitic Complex. Thus, its age can be preliminarily assumed to correspond to the latest Triassic. However, due to the very restricted spatial distribution and the lack of biostratigraphical markers, the precise age of the discussed sediments remains contested.

An age of about 198 Ma was proposed by a geochronological study ($^{40}Ar/^{39}Ar$) of the lava flows outcropping the western Algarve (Verati *et al.* 2007). However, Callegaro *et al.* (2014) recalibrated those results, indicating the age of 199.7 ± 1.4 Ma. The basaltic and volcanoclastic levels outcropping in the studied Rocha da Pena area were not absolutely dated, but based on samples analysed in nearby sites, they are most likely the latest Triassic—earliest Jurassic in age (Verati *et al.* 2007; Pérez-López 2021).

Conclusions

This study examines a 28-metre-thick stratigraphical sequence at Rocha da Pena, situated within the upper Silves Group, providing new geological and palaeontological insights into the Late Triassic successions of southern Portugal. Detailed sedimentological analysis has led to the identification of six distinct facies associations, which are grouped into three lithological units.

The sedimentological evidence indicates a predominantly low-energy depositional system. The mudstone–carbonate succession, part of the Silves Marl–Carbonate Evaporitic Complex, comprises mudstone, calcrete, and palustrine facies. These deposits are interpreted as having developed in coastal alluvial mudflats affected by ephemeral and/or seasonally fluctuating water bodies, under semi-arid conditions. The interplay of subaerial exposure, pedogenesis, and periodic flooding resulted in a complex facies mosaic and notable textural variability.

The siltstone and sandstone deposits, tentatively attributed to the uppermost part of the Silves Marl–Carbonate Evaporitic Complex, are interpreted as having formed in marginal and tidally-influenced environments. Volcanoclastic and volcanic layers, assigned to the Volcano-Sedimentary Series, are present at the top of the studied succession and are associated with the early stages of CAMP volcanism.

Novel fossil material recovered from the mudstone facies includes unionid bivalves and isolated actinopterygian scales. These remains were found in proximity to a *Metoposaurus* bonebed. The origin of this bonebed is preliminarily suggested as a result of likely biogenic aggregation followed by the disarticulation of skeletal elements during subsequent flooding.

Additional fossil-bearing layers have been identified within the palustrine carbonate and calcrete facies. Although the material is generally fragmented and poorly preserved due to intense pedogenetic and diagenetic alteration, some identifiable remains were recovered. These include cyamodontoid placodont armor plates, actinopterygian scales, and the first Triassic record of hybodont sharks in Portugal, represented by a fin spine.

Faunal assemblages vary notably between facies. Fossils from the mudstone facies preserve a freshwater fauna indicated by the unionid bivalves. In contrast, the palustrine facies are dominated by placodont remains, with no diagnostic freshwater taxa present. These differences may reflect environmental variation, particularly in salinity, but may also be influenced by sampling bias. Thus, further research is required to better understand the link between facies and faunal assemblages.

Although the Silves Marl–Carbonate Evaporitic Complex has recently been dated to span from the upper Carnian to the latest Rhaetian/lowermost Hettangian, the precise age of the vertebrate-bearing horizons remains unresolved. The absence of palynological data and biostratigraphically informative invertebrate fossils limits chronological resolution. While the recovered tetrapod fauna, including *Metoposaurus*, a basal phytosaur, and *Henodus*, is most consistent with a Carnian age, the stratigraphical position of the fossiliferous horizons near the top of the Silves Group may point to a younger age. At present, the available data do not permit definitive conclusions regarding the age of these deposits.

Acknowledgements.- We thank the two anonymous reviewers and Grzegorz Niedźwiedzki for their constructive and very helpful comments, enhancing the quality of the manuscript. We thank Franciso Lopes for sharing his thesis and observations on Rocha da Pena geology. We would also like to thank Anthonie Hellemond for help during fieldwork. Funding: Câmara Municipal de Loulé, R & D Unit GEOBIOTEC - UID/04035: GeoBioCiências, GeoTecnologias e GeoEngenharias.

References

Alonso-Zarza, A.M. 1999: Initial stages of laminar calcrete formation by roots: examples from the Neogene of central Spain. *Sedimentary Geology 126*, 177–191. https://doi.org/10.1016/S0037-0738(99)00039-1

Alonso-Zarza, A.M. 2003; Palaeoenvironmental significance of palustrine carbonates and calcretes in the geological record. *Earth-Science Reviews 60*, 261–298. https://doi.org/10.1016/S0012-8252(02)00106-X

Alonso-Zarza, A.M. & Wright, V.P. 2010; *Calcretes*. *In* Alonso-Zarza A.M. & Tanner L.H. (eds), *Developments in Sedimentology 61*. Elsevier, 225–267. https://doi.org/10.1016/S0070-4571(09)06105-6

Alonso-Zarza, A.M., Calvo, J.P. & García del Cura, M.A. 1992: Palustrine sedimentation and associated features—grainification and pseudo-microkarst—in the Middle Miocene (intermediate unit) of the Madrid Basin, Spain. *Sedimentary Geology 76*, 43–61. https://doi.org/10.1016/0037-0738(92)90138-H

Ambrosetti, E., Martini, I. & Sandrelli, F. 2017: Shoal-water deltas in high-accommodation settings: Insights from the lacustrine Valimi Formation (Gulf of Corinth, Greece). *Sedimentology 64*, 425–452. https://doi.org/10.1111/sed.12309

Antczak, M. & Bodzioch, A. 2018: Diversity of Fish Scales in Late Triassic Deposits of Krasiejów (SW Poland). *Paleontological Research 22*, 91–100. https://doi.org/10.2517/2017PR012

Arche, A. & López-Gómez, J. 2014: The Carnian Pluvial Event in Western Europe: New data from Iberia and correlation with the Western Neotethys and Eastern North America–NW Africa regions. *Earth-Science Reviews 128*, 196–231. https://doi.org/10.1016/j.earscirev.2013.10.012

Archer, S. G., McKie, T., Andrews, S. D., Wilkins, A. D., Hutchison, M., Young-Ziolkowski, N., Osunde, C., Matheson, J., Thackrey, S., Lang, M., Sola, B., Mouritzen, C., Perrell, C., Greenwood, M., Mauritzen, E. & Tenepalli, S. 2022: Triassic mudstones of the Central North Sea: cross-border characterization, correlation and their palaeoclimatic significance. In: *Cross-Border Themes in Petroleum Geology I: The North Sea*. Geological Society of London, 333–378. https://doi.org/10.1144/SP494-2019-61

Azerêdo, A.C., Duarte, L.V., Henriques, M.H., & Manuppella, G. 2003: *Da Dinâmica Continental no Triásico aos Mares do Jurássico Inferior e Médio*. Instituto Geológico e Mineiro, Lisbon.

Bahr, A., Kolber, G., Kaboth-Bahr, S., Reinhardt, L., Friedrich, O. & Pross, J. 2020: Mega-monsoon variability during the late Triassic: Re-assessing the role of orbital forcing in the deposition of playa sediments in the Germanic Basin. *Sedimentology 67*, 951–970. https://doi.org/10.1111/sed.12668

Bao, H., Koch, P.L. & Hepple, R.P. 1998: Hematite and calcite coatings on fossil vertebrates. *Journal of Sedimentary Research 68*, 727–738. https://doi.org/10.2110/jsr.68.727

Bayet-Goll, A. & Neto de Carvalho, C. 2016: Ichnology and sedimentology of a tide-influenced delta in the Ordovician from the northeastern Alborz range of Iran (Kopet Dagh region). *Lethaia 49,* 327–350. https://doi.org/10.1111/let.12150

Behrensmeyer, A.K. 1978: Taphonomic and ecologic information from bone weathering. *Paleobiology 4*, 150–162. https://doi.org/10.1017/S0094837300005820

Benton, M.J. & Wu, F. 2022: Triassic Revolution. *Frontiers in Earth Science 10*. https://doi.org/10.3389/feart.2022.899541

Bodzioch, A. & Kowal-Linka, M. 2012: Unraveling the origin of the Late Triassic multitaxic bone accumulation at Krasiejów (S Poland) by diagenetic analysis. *Palaeogeography, Palaeoclimatology, Palaeoecology 346–347*, 25–36. https://doi.org/10.1016/j.palaeo.2012.05.015

Bogan, A. & Weaver, P. 2012: A new genus and new species of freshwater mussel from the Late Triassic rift lakes of eastern North Carolina (Mollusca: Bivalvia: Unionida: cf. Unionidae). *The Nautilus 126*, 105–112.

Bonnet, C. 1850: *Algarve. Description Géographique et Geólogique de Cette Province, par Charles Bonnet.* Ouvrage approuvé et imprimé par l'Académie Royale des Sciences de Lisbonne, Lisbon.

Braithwaite, C.J.R. 2023: Controls on carbonate-siliciclastic relationships in Quaternary deposits of the Midyan coast of the Gulf of Aqaba, Saudi Arabia. *Marine Geology 456*, 106985. https://doi.org/10.1016/j.margeo.2022.106985

Breda, A. & Preto, N. 2011: Anatomy of an Upper Triassic continental to marginal-marine system: the mixed siliciclastic–carbonate Travenanzes Formation (Dolomites, Northern Italy). *Sedimentology 58*, 1613–1647. https://doi.org/10.1111/j.1365-3091.2011.01227.x

Brinkman, D.B., Eberth, D.A. & Currie, P.J. 2007: From bonebeds to paleobiology: applications of bonebed data. *In:* Rogers, R.R., Eberth, D.A. & Fiorillo, A.R. (eds), *Bonebeds: Genesis, Analysis, and Paleobiological Significance,* 221–263. University of Chicago Press, Chicago.

Brownstein, C.D. 2023: A late-surviving phytosaur from the northern Atlantic rift reveals climate constraints on Triassic reptile biogeography. *BMC Ecology and Evolution 23*, 33. https://doi.org/10.1186/s12862-023-02136-8

Brusatte, S.L., Butler, R.J., Mateus, O. & Steyer, J. S. 2015: A new species of *Metoposaurus* from the Late Triassic of Portugal and comments on the systematics and biogeography of metoposaurid temnospondyls. *Journal of Vertebrate Paleontology 35*, e912988. https://doi.org/10.1080/02724634.2014.912988

Buffa, V., Jalil, N.-E. & Steyer, J.S. 2019: Redescription of *Arganasaurus* (*Metoposaurus*) *azerouali* (Dutuit) comb. nov. from the Upper Triassic of the Argana Basin (Morocco), and the first phylogenetic analysis of the Metoposauridae (Amphibia, Temnospondyli). *Papers in Palaeontology 5*, 699–717. https://doi.org/10.1002/spp2.1259

Bustillo, M.A., Armenteros, I. & Huerta, P. 2017: Dolomitization, gypsum calcitization and silicification in carbonate–evaporite shallow lacustrine deposits. *Sedimentology 64*, 1147–1172. https://doi.org/10.1111/sed.12345

Butler, R.J., Jones, A.S., Buffetaut, E., Mandl, G.W., Scheyer, T.M. & Schultz, O. 2019: Description and phylogenetic placement of a new marine species of phytosaur (Archosauriformes: Phytosauria) from the Late Triassic of Austria. *Zoological Journal of the Linnean Society 187*, 198–228. https://doi.org/10.1093/zoolinnean/zlz014

Callegaro, S., Rapaille, C., Marzoli, A., Bertrand, H., Chiaradia, M., Reisberg, L., Bellieni, G., Martins, L., Madeira, J., Mata, J., Youbi, N., De Min, A., Azevedo, M.R., & Bensalah, M.K. 2014: Enriched mantle source for the Central Atlantic magmatic province: New supporting evidence from southwestern Europe. *Lithos 188*, 15–32. https://doi.org/10.1016/j.lithos.2013.10.021

Carracedo, M., Sarrionandia, F., Juteau, T. & Ibarguchi, J. 2012: Structure and organization of submarine basaltic flows: Sheet flow transformation into pillow lavas in shallow submarine environments. *International Journal of Earth Sciences 101*. https://doi.org/10.1007/s00531-012-0783-2

Carrillo-Briceño, J.D., Cadena, E.A., Dececchi, A.T., Larson, H.C.E. & Du, T.Y. 2016: First record of a hybodont shark (Chondrichthyes: Hybodontiformes) from the Lower Cretaceous of Colombia. *Neotropical Biodiversity 2*, 81–86. https://doi.org/10.1080/23766808.2016.1191749

Cavin, L. 2017: *Freshwater Fishes: 250 Million Years of Evolutionary History*. ISTE Press, Elsevier, London.

Chen, S., Guo, Z., Pe-Piper, G. & Zhu, B. 2013: Late Paleozoic peperites in West Junggar, China, and how they constrain

regional tectonic and palaeoenvironmental setting. *Gondwana Research 23*, 666–681. https://doi.org/10.1016/j.gr.2012.04.012

Cherns, L., Wheeley, J. R. & Wright, V. P. 2010: Taphonomic Bias in Shelly Faunas Through Time: Early Aragonitic Dissolution and Its Implications for the Fossil Record. *In:* Allison, P.A. & Bottjer, D.J. (eds) *Taphonomy. Aims & Scope Topics in Geobiology Book Series 32*. Springer, Dordrecht. https://doi.org/10.1007/978-90-481-8643-3_3

Cherns, L. & Wright, V.P. 2009: Quantifying the impacts of early diagenetic aragonite dissolution on the fossil record. *Palaios 24*, 756–771. https://doi.org/10.2110/palo.2008.p08-134r

Choffat, P. 1887: *Recherches sur les terrains secondaires au Sud du Sado*. Commissão dos Trabalhos Geológicos de Portugal, Lisbon.

Costantini, E.A.C., Lessovaia, S. & Vodyanitskii, Y. 2006: Using the analysis of iron and iron oxides in paleosols (TEM, geochemistry and iron forms) for the assessment of present and past pedogenesis. *Quaternary International 156–157*, 200–211. https://doi.org/10.1016/j.quaint.2006.05.008

Daidu, F., Yuan, W. & Min, L. 2013: Classifications, sedimentary features and facies associations of tidal flats. *Journal of Palaeogeography 2*, 66–80. https://doi.org/10.3724/SP.J.1261.2013.00018

Danise, S., Cavalazzi, B., Dominici, S., Westall, F., Monechi, S. & Guioli, S. 2012: Evidence of microbial activity from a shallow water whale fall (Voghera, northern Italy). *Palaeogeography, Palaeoclimatology, Palaeoecology 317–318*, 13–26. https://doi.org/10.1016/j.palaeo.2011.12.001

Datta, D. & Ray, S. 2023: A giant phytosaur (Diapsida, Archosauria) from the Upper Triassic of India with new insights on phytosaur migration, endemism and extinction. *Papers in Palaeontology 9*, e1476. https://doi.org/10.1002/spp2.1476

Davies, J.H.F.L., Marzoli, A., Bertrand, H., Youbi, N., Ernesto, M. & Schaltegger, U. 2017: End-Triassic mass extinction started by intrusive CAMP activity. *Nature Communications 8*, 15596. https://doi.org/10.1038/ncomms15596

Davis, R.A. 2012: Tidal Signatures and Their Preservation Potential in Stratigraphic Sequences. *In:* Davis, R.A. & Dalrymple, R.W. (eds), *Principles of Tidal Sedimentology*. Springer Dordrecht, 35–55. https://doi.org/10.1007/978-94-007-0123-6_3

Dinis, P.A., Fernandes, P., Jorge, R.C.G.S., Rodrigues, B., Chew, D. M. & Tassinari, C. G. 2018: The transition from Pangea amalgamation to fragmentation: Constraints from detrital zircon geochronology on West Iberia paleogeography and sediment sources. *Sedimentary Geology 375*, 172–187. https://doi.org/10.1016/j.sedgeo.2017.09.015

Debret, M., Sebag, D., Desmet, M., Balsam, W., Copard, Y., Mourier, B., Susperrigui, A. S., Arnaud, F., Bentaleb, I., Chapron, E., Lallier-Vergès, E. & Winiarski, T. 2011: Spectrocolorimetric interpretation of sedimentary dynamics: The new 'Q7/4 diagram'. *Earth-Science Reviews 109*, 1–19. https://doi.org/10.1016/j.earscirev.2011.07.002

de Miguel Chaves, C., Scheyer, T. M., Ortega, F. & Pérez-García, A. 2020: The placodonts (Sauropterygia) from the Middle Triassic of Canales de Molina (Central Spain), and an update on the knowledge about this clade in the Iberian record. *Historical Biology 32*, 34–48. https://doi.org/10.1080/08912963.2018.1462805

Dubiel, R.F. & Hasiotis, S.T. 2011: Deposystems, paleosols, and climatic variability in a continental system: the Upper Triassic Chinle Formation, Colorado Plateau, USA. *In:* Davidson, S.K., Leleu, S. & North C.P. (eds), *From River to Rock Record* 97. Society for Sedimentary Geology (SEPM), Special Publication. https://doi.org/10.2110/sepmsp.097.393

Dzik, J. & Sulej, T. 2007: A review of the early Late Triassic Krasiejów biota from Silesia, Poland. *Palaeontologia Polonica 64*, 3–27.

Eckardt, F.D., Drake, N., Goudie, A.S., White, K. & Viles, H. 2001: The role of playas in pedogenic gypsum crust formation in the Central Namib Desert: a theoretical model. *Earth Surface Processes and Landforms 26*, 1177–1193. https://doi.org/10.1002/esp.264

Fernandez-Jalvo, Y. & Andrews, P. 2016: *Atlas of Taphonomic Identifications: 1001+ Images of Fossil and Recent Mammal Bone Modification*. Springer Dordrecht.

Flügel, E. & Munnecke, A. 2010: *Microfacies of Carbonate Rocks: Analysis, Interpretation and Application*. Springer Berlin, Heidelberg.

Freytet, P. & Verrecchia, E. P. 2002: Lacustrine and palustrine carbonate petrography: an overview. *Journal of Paleolimnology 27*, 221–237. https://doi.org/10.1023/A:1014263722766

Gama, C., Pereira, M.F., Crowley, Q.G., Dias da Silva, Í. & Silva, J.B. 2021: Detrital zircon provenance of Triassic sandstone of the Algarve Basin (SW Iberia): evidence of Gondwanan- and Laurussian-type sources of sediment. *Geological Magazine 158*, 311–329. https://doi.org/10.1017/S0016756820000370

García-Ávila, M., De la Horra, R., de Miguel Chaves, C., Juncal, M.A., Pérez-García, A., Ortega, F. & Diez, J. B. 2021: Palynological and sedimentological implications of the sauropterygian Upper Triassic site of El Atance (Central Iberian Peninsula). *Review of Palaeobotany and Palynology 295*, 104541. https://doi.org/10.1016/j.revpalbo.2021.104541

Gierlowski-Kordesch, E.H. 2010: Lacustrine Carbonates. In: Alonso-Zarza, A.M. & Tanner, L.H. (eds), *Developments in Sedimentology* 61. Elsevier. https://doi.org/10.1016/S0070-4571(09)06101-9

Goodbred, S.L., Saito, Y. 2012: Tide-Dominated Deltas. *In:* Davis, R. Jr. & Dalrymple, R. (eds), *Principles of Tidal Sedimentology*. Springer, Dordrecht, 129–149. https://doi.org/10.1007/978-94-007-0123-6_7

Godfree, R.C., Knerr, N., Godfree, D., Busby, J., Robertson, B., & Encinas-Viso, F. 2019: Historical reconstruction unveils the risk of mass mortality and ecosystem collapse during pancontinental megadrought. *Proceedings of the National Academy of Sciences 116*. https://doi.org/10.1073/pnas.1902046116

Golonka, J. 2007: Late Triassic and Early Jurassic palaeogeography of the world. *Palaeogeography, Palaeoclimatology, Palaeoecology 244*, 297-307. https://doi.org/10.1016/j.palaeo.2006.06.041

Goy, A.G. & Aliaga, A.M. 1998: Bivalvos del Triásico Superior en la Formación Imón (Cordillera Ibérica, España). *Boletín de la Real Sociedad Española de Historia Natural. Sección Geológica 94*, 77–91.

Gray, M.B. & Nickelsen, R.P. 1989: Pedogenic slickensides, indicators of strain and deformation processes in redbed sequences of the Appalachian foreland. *Geology 17*, 72–75. https://doi.org/10.1130/0091-7613(1989)017<0072:PSIOSA>2.3.CO;2

Haag, W.R. & Warren, M.L. 2008: Effects of Severe Drought on Freshwater Mussel Assemblages. *Transactions of the American Fisheries Society 137*, 1165–1178. https://doi.org/10.1577/T07-100.1

Hausmann, I.M., Nuetzel, A., Roden, V.J. & Reich, M. 2021: Palaeoecology of tropical marine invertebrate assemblages from the Late Triassic of Misurina, Dolomites, Italy. *Acta Palaeontologica Polonica 66*, 143–192. https://doi.org/10.4202/app.00659.2019

Heckert, A. 2004: Late Triassic microvertebrates from the lower Chinle Group (Otischalkian-Adamanian: Carnian), southwestern U.S.A. *New Mexico Museum of Natural History and Science Bulletin 27*, 1–170.

Heckert, A., Mitchell, J., Schneider, V. & Olsen, P. 2012: Diverse New Microvertebrate Assemblage from the Upper Triassic Cumnock Formation, Sanford Subbasin, North Carolina, USA. *Journal of Paleontology 86*, 368–390. https://doi.org/10.2307/41480198

Helfman, G.S., Collette, B.B., Facey, D.E. & Bowen, B.W. 2009: *The Diversity of Fishes: Biology, Evolution, and Ecology*. Wiley, Oxford.

Huerta, P., Armenteros, I., Recio, C., & Blanco, J.A. 2010: Palaeogroundwater evolution in playa–lake environments: Sedimentary facies and stable isotope record (Palaeogene, Almazán basin, Spain). *Palaeogeography, Palaeoclimatology,*

Palaeoecology 286, 135–148. https://doi.org/10.1016/j.palaeo.2009.12.008

Huerta, P., Armenteros, I., & Silva, P.G. 2011: Large-scale architecture in non-marine basins: the response to the interplay between accommodation space and sediment supply. *Sedimentology 58*, 1716-1736. https://doi.org/10.1111/j.1365-3091.2011.01231.x

Hughes, Z.J. 2012: Tidal Channels on Tidal Flats and Marshes. *In:* Davis, R. Jr. & Dalrymple, R. (eds), *Principles of Tidal Sedimentology*. Springer, Dordrecht, 269–300. https://doi.org/10.1007/978-94-007-0123-6_11

Jewuła, K., Matysik, M., Paszkowski, M. & Szulc, J. 2019: The late Triassic development of playa, gilgai floodplain, and fluvial environments from Upper Silesia, southern Poland. *Sedimentary Geology 379*, 25–45. https://doi.org/10.1016/j.sedgeo.2018.11.005

Jewuła, K., Trela, W., Wasielka, N. & Archer, S.G. 2023: Palustrine limestones and calcretes as the sedimentary record of paleoenvironmental changes in a Late Permian semi-arid climate at the SE periphery of the Southern Permian Basin (the Holy Cross Mountains, Poland). *Palaeogeography, Palaeoclimatology, Palaeoecology 614*, 111398. https://doi.org/10.1016/j.palaeo.2023.111398

Jorge, R.C.G.S., Fernandes, P., Rodrigues, B., Pereira, Z. & Oliveira, J.T. 2013: Geochemistry and provenance of the Carboniferous Baixo Alentejo Flysch Group, South Portuguese Zone. *Sedimentary Geology 284–285*, 133–148. https://doi.org/10.1016/j.sedgeo.2012.12.005

Khalloufi, B. & Jalil, N.-E. 2020: Overview of the Late Triassic (Carnian) actinopterygian fauna from the Argana Basin (Morocco). *Comptes Rendus Géoscience 352*, 495–513. https://doi.org/10.5802/crgeos.34

Kim, S.-H., Lee, Y.-N., Park, J.-Y., Lee, S. & Lee, H.-J. 2020: The first record of redfieldiiform fish (Actinopterygii) from the Upper Triassic of Korea: Implications for paleobiology and paleobiogeography of Redfieldiiformes. *Gondwana Research 80*, 275–284. https://doi.org/10.1016/j.gr.2019.11.008

Klappa, C.F. 1980: Rhizoliths in terrestrial carbonates: classification, recognition, genesis and significance. *Sedimentology 27*, 613–629. https://doi.org/10.1111/j.1365-3091.1980.tb01651.x

Kovalchuk, O.M. & Anfimova, G.V. 2020: Lepisosteiform fish (Holostei) ganoid scales from the middle Jurassic deposits of Ukraine. *Zoodiversity 54*. https://doi.org/10.15407/zoo2020.01.035

Kowal-Linka, M. 2015: Analysis of marrow cavity fillings as a tool to recognise diverse taphonomic histories of fossil reptile bones: Implications for the genesis of the Lower Muschelkalk marine bone-bearing bed (Middle Triassic, Żyglin, S Poland). *Palaeogeography, Palaeoclimatology, Palaeoecology 436*, 64–76. https://doi.org/10.1016/j.palaeo.2015.06.040

Kowalski, J., Bodzioch, A., Janecki, P., Ruciński, M. & Antczak, M. 2019: Preliminary report on the microvertebrate faunal remains from the Late Triassic locality at Krasiejów, SW Poland. *Annales Societatis Geologorum Poloniae* 89. https://doi.org/10.14241/asgp.2019.10

Kraus, M.J. 1999: Paleosols in clastic sedimentary rocks: their geologic applications. *Earth-Science Reviews 47*, 41–70. https://doi.org/10.1016/S0012-8252(99)00026-4

Kraus, M.J., & Aslan, A. 1995: Palaeosol sequences in floodplain environments: a hierarchical approach. In: Thiry, M. & Simon-Coinçon, M. (eds), *Palaeoweathering, Palaeosurfaces and Related Continental Deposits*. International Association of Sedimentologists Special Publication 27, 303–321. https://doi.org/10.1002/9781444304190.ch12

Kraus, M.J. & Hasiotis, S.T. 2006: Significance of different modes of rhizolith preservation to interpreting paleoenvironmental and paleohydrologic settings: examples from Paleogene paleosols, Bighorn Basin, Wyoming, USA. *Journal of Sedimentary Research 76*, 633–646. https://doi.org/10.2110/jsr.2006.052

Kufner, A.M., Deckman, M.E., Miller, H.R., So, C., Price, B.R. & Lovelace, D.M. 2025: A new metoposaurid (Temnospondyli) bonebed from the lower Popo Agie Formation (Carnian, Triassic) and an assessment of skeletal sorting. *PloS One 20*, e0317325. https://doi.org/10.1371/journal.pone.0317325

Kvale, E.P. 2012: Tidal Constituents of Modern and Ancient Tidal Rhythmites: Criteria for Recognition and Analyses. *In:* Davis. R. Jr. & Dalrymple, R. (eds), *Principles of Tidal Sedimentology*, 1–17. Springer, Dordrecht. https://doi.org/10.1007/978-94-007-0123-6_1

Leleu, S., Hartley, A.J., van Oosterhout, C., Kennan, L., Ruckwied, K., & Gerdes, K. 2016: Structural, stratigraphic and sedimentological characterisation of a wide rift system: the Triassic rift system of the Central Atlantic Domain. *Earth-Science Reviews 158*, 89–124. https://doi.org/10.1016/j.earscirev.2016.03.008

Leuzinger, L., Cuny, G., Popov, E. & Billon-Bruyat, J.-P. 2017: A new chondrichthyan fauna from the Late Jurassic of the Swiss Jura (Kimmeridgian) dominated by hybodonts, chimaeroids and guitarfishes. *Papers in Palaeontology 3*, 471–511. https://doi.org/10.1002/spp2.1085

Lopes, F. 2014: Novas interpretações do Triásico da parte central da Bacia do Algarve (Portugal). *Comunicações Geológicas 101*.

López-Gómez, J. *et al.* 2019: Permian-Triassic Rifting Stage. *In:* Quesada, C. & Oliveira, J. (eds) *The Geology of Iberia: A Geodynamic Approach. Regional Geology Reviews*, 29–112. Springer, Cham. https://doi.org/10.1007/978-3-030-11295-0_3

López-Rojas, V., Moreno-Azanza, M. and Puértolas-Pascual, E. 2025: Systematic utility of the phytosaur post-dentary mandibular region. *Papers in Palaeontology* 11: e70045. https://doi.org/10.1002/spp2.70045

Lucas, S. 2020: Biochronology of Late Triassic Metoposauridae (Amphibia, Temnospondyli) and the Carnian pluvial episode. *Annales Societatis Geologorum Poloniae 90*. https://doi.org/10.14241/asgp.2020.29

Lucas, S.G., Rinehart, L.F., Krainer, K., Spielmann, J.A. & Heckert, A.B. 2010: Taphonomy of the Lamy amphibian quarry: A Late Triassic bonebed in New Mexico, U.S.A. *Palaeogeography, Palaeoclimatology, Palaeoecology 298*, 388–398. https://doi.org/10.1016/j.palaeo.2010.10.025

Mack, G.H., James, W.C. & Monger, H.C. 1993: Classification of paleosols. *Geological society of America Bulletin 105*, 129–136. https://doi.org/10.1130/0016-7606(1993)105<0129:COP>2.3.CO;2

MacNeil, A.J. & Jones, B. 2006: Palustrine deposits on a Late Devonian coastal plain —sedimentary attributes and implications for concepts of carbonate sequence stratigraphy. *Journal of Sedimentary Research 76*, 292–309. https://doi.org/10.2110/jsr.2006.028

Maisey, J.G. 1978: Growth and form of finspines in hybodont sharks. *Palaeontology 21*, 657–666.

Maisey, J.G. 1982: The anatomy and interrelationships of Mesozoic hybodont sharks. *American Museum Novitates 2724*, 1–48.

Manuppella, G. 1992: *Carta Geológica da Região do Algarve.* [2 sheets at the 1:100.000 scale and Explanatory Note.]. Serviços Geológicos de Portugal.

Mancuso, A.C., & Previtera, E. 2022: Bone diagenesis of tetrapods from the Middle Triassic Tarjados Formation: implication for depositional environment and palaeoclimate. *Palaeobiodiversity and Palaeoenvironments 102*, 205–221. https://doi.org/10.1007/s12549-021-00500-4

Mancuso, A.C., Previtera, E., Benavente, C.A. & Del Pino, S.H. 2017: Evidence of bacterial decay and early diagenesis in a partially articulated tetrapod from the Triassic Chañares Formation. *Palaios 32*, 367–381. https://doi.org/10.2110/palo.2016.076

Manzanares, E., Pla, C., Ferrón, H.G., & Botella, H. 2018: Middle-Late Triassic chondrichthyans remains from the Betic Range (Spain). *Journal of Iberian Geology 44*, 129–138. https://doi.org/10.1007/s41513-017-0027-1

Manzanares, E., Pla, C., Martínez-Pérez, C., Ferrón, H., & Botella, H. 2017: *Lonchidion derenzii*, sp. nov., a new lonchidiid shark (Chondrichthyes, Hybodontiforms) from the Upper Triassic of Spain, with remarks on lonchidiid enameloid. *Journal of Vertebrate Paleontology 37*, e1253585. https://doi.org/10.1080/02724634.2017.1253585

Marriott, S.B. & Wright, V.P. 1993: Palaeosols as indicators of geomorphic stability in two Old Red Sandstone alluvial suites, South Wales. *Journal of the Geological Society 150,* 1109–1120. https://doi.org/10.1144/gsjgs.150.6.1109

Marriott, S.B., & Wright, V.P. 2006: Investigating paleosol completeness and preservation in mid-Paleozoic alluvial paleosols: a case study in paleosol taphonomy from the Lower Old Red Sandstone. *In:* Alonso-Zarza, A.M. & Tanner, L.H. (eds), *P aleoenvironmental Record and Applications of Calcretes and Palustrine Carbonates*. Geological Society of America, Boulder. https://doi.org/10.1130/2006.2416(03)

Martin, U. & Nemeth, K. 2007: Blocky versus fluidal peperite textures developed in volcanic conduits, vents and crater lakes of phreatomagmatic volcanoes in Mio/Pliocene volcanic fields of Western Hungary. *Journal of Volcanology and Geothermal Research 159*, 164–178. https://doi.org/10.1016/j.jvolgeores.2006.06.010

Martinius, A.W. 2012: Contrasting styles of siliciclastic tidal deposits in a developing thrust-sheet-top basins – the Lower Eocene of the Central Pyrenees (Spain). *In:* Davis, R. Jr., & Dalrymple, R. (eds), *Principles of Tidal Sedimentology,* 473–506. Springer, Dordrecht. https://doi.org/10.1007/978-94-007-0123-6_18

Martins, L.T., Madeira, J., Youbi, N., Munhá, J., Mata, J. & Kerrich, R. 2008: Rift-related magmatism of the Central Atlantic magmatic province in Algarve, Southern Portugal. *Lithos 101*, 102–124. https://doi.org/10.1016/j.lithos.2007.07.010

Marty, D. & Meyer, C.A. 2006: Depositional conditions of carbonate-dominated palustrine sedimentation around the KT boundary (Facies Rognacien, northeastern Pyrenean foreland, southwestern France). *GSA Special Paper 416*, 169–187. https://doi.org/10.1130/2006.2416(11)

Marzoli, A., Renne, P.R., Piccirillo, E.M., Ernesto, M., Bellieni, G. & de Min, A. 1999: Extensive 200-million-year-old continental flood basalts of the Central Atlantic Magmatic Province. *Science 284*, 616-618. https://doi.org/10.1126/science.284.5414.616

Mateus, O., Butler, R.J., Brusatte, S.L., Whiteside, J.H. & Steyer, J. S. 2014: The first phytosaur (Diapsida, Archosauriformes) from the Late Triassic of the Iberian Peninsula. *Journal of Vertebrate Paleontology 34*, 970–975. https://doi.org/10.1080/02724634.2014.840310

Matthews, W.J. & Marsh-Matthews, E. 2003: Effects of drought on fish across axes of space, time and ecological complexity. *Freshwater Biology 48*, 1232–1253. https://doi.org/10.1046/j.1365-2427.2003.01087.x

Mayoral, E.J., Santos, A. & Diez, B. 2016: First evidence of rooting lycopsids preserved as imprints and trace fossils from the Silves Sandstone (Upper Triassic, eastern Algarve, South Portugal). *Spanish Journal of Palaeontology 31*, 131–143. https://doi.org/10.7203/sjp.31.1.17143

Mazumder, R. & Arima, M. 2005: Tidal rhythmites and their implications. *Earth-Science Reviews 69*, 79–95. https://doi.org/10.1016/j.earscirev.2004.07.004

Mears, E.M., Rossi, V., Macdonald, E., Coleman, G., Davies, T.G., Arias-Riesgo, C., Hildebrandt, C., Thiel, H., Duffin, C.J., Whiteside, D.I., & Benton, M.J. 2016: The Rhaetian (Late Triassic) vertebrates of Hampstead Farm Quarry, Gloucestershire, UK. *Proceedings of the Geologists' Association 127*, 478–505. https://doi.org/10.1016/j.pgeola.2016.05.003

Mellere, D., Mannie, A., Longhitano, S., Mazur, M., Kulausa, H., Brough, S. & Cotton, J. 2017: *Tidally Influenced Shoal Water Delta and Estuary in the Middle Jurassic of the Søgne Basin, Norwegian North Sea: Sedimentary Response to Rift Initiation and Salt Tectonics.* Geological Society, London, Special Publications 444, 173–213. https://doi.org/10.1144/SP444.11

Milner, A.R. & Schoch, R.R. 2004: The latest metoposaurid amphibians from Europe. *Neues Jahrbuch für Geologie und Paläontologie-Abhandlungen* 231–252.

Milroy, P., Wright, V.P. & Simms, M.J. 2019: Dryland continental mudstones: Deciphering environmental changes in problematic mudstones from the Upper Triassic (Carnian to Norian) Mercia Mudstone Group, south-west Britain. *Sedimentology 66*, 2557–2589. https://doi.org/10.1111/sed.12626

Moreno, R., Chakravorti, S., Cooper, S.L. & Schoch, R.R. 2024: Unexpected temnospondyl diversity in the early Carnian Grabfeld Formation (Germany) and the palaeogeography of metoposaurids. *Fossil Record 27*, 381–400. https://doi.org/10.3897/fr.27.121996

Munnecke, A., Westphal, H., Reijmer, J.J.G. & Samtleben, C. 1997: Microspar development during early marine burial diagenesis: a comparison of Pliocene carbonates from the Bahamas with Silurian limestones from Gotland (Sweden). *Sedimentology 44*, 977–990. https://doi.org/10.1111/j.1365-3091.1997.tb02173.x

Nomade, S., Knight, K.B., Beutel, E., Renne, P.R., Verati, C., Féraud, G., Marzoli, A., Youbi, N., & Bertrand, H. 2007: Chronology of the Central Atlantic Magmatic Province: Implications for the Central Atlantic rifting processes and the Triassic–Jurassic biotic crisis. *Palaeogeography, Palaeoclimatology, Palaeoecology 244*, 326–344. https://doi.org/10.1016/j.palaeo.2006.06.034

Onézime, J., Charvet, J., Faure, M., Bourdier, J.-L. & Chauvet, A. 2003: A new geodynamic interpretation for the South Portuguese Zone (SW Iberia) and the Iberian Pyrite Belt genesis. *Tectonics 22*. https://doi.org/10.1029/2002TC001387

Ortí, F., Pérez-López, A. & Salvany, J.M. 2017: Triassic evaporites of Iberia: Sedimentological and palaeogeographical implications for the western Neotethys evolution during the Middle Triassic–Earliest Jurassic. *Palaeogeography, Palaeoclimatology, Palaeoecology 471*, 157–180. https://doi.org/10.1016/j.palaeo.2017.01.025

Palain, C. 1968a: Analyse séquentielle et lithostratigraphique de la série de base du Mésozoique portugais au Nord du Tage. *Académie des Sciences Verfasser 480*, xx–xx.

Palain, C. 1968b: Preuves paléontologiques de l'existence de Keuper au Portugal, dans la province de I 'Algarve. *Comptes Rendus Hebdomadaires Des Séances De L'Académie Des Sciences Série D 267*, xx–xx.

Palain, C. 1976: Une série détritique terrigène les 'Grès de Silves': Trias et Lias inférieur du Portugal. *Memória dos Serviços Geológicos de Portugal, Nova Série 25*, xx–xx.

Palain, C. 1979: Connaissances stratigraphiques sur la base du Mésozoique portugais. *Ciências da Terra Univ Nova Lisboa 5*, 11–28.

Panfili, G., Cirilli, S., Corso, J.D., Bertrand, H., Medina, F., Youbi, N. & Marzoli, A. 2019: New biostratigraphic constraints show rapid emplacement of the Central Atlantic Magmatic Province (CAMP) during the end-Triassic mass extinction interval. *Global and Planetary Change 172*, 60–68. https://doi.org/10.1016/j.gloplacha.2018.09.009

Parrish, J. 1993: Climate of the Supercontinent Pangea. *Journal of Geology 101*, 215–233. https://doi.org/10.1086/648217

Pasierbiewicz, K.W. 1982: Experimental study of cross-strata development on an undulatory surface and implications relative to the origin of flaser and wavy bedding. *Journal of Sedimentary Research 52*, 769–778. https://doi.org/10.1306/212F8049-2B24-11D7-8648000102C1865D

Pawlak, W., Rozwalak, P. & Sulej, T. 2022: Triassic fish faunas from Miedary (Upper Silesia, Poland) and their implications for understanding paleosalinity. *Palaeogeography, Palaeoclimatology, Palaeoecology 590*, 110860. https://doi.org/10.1016/j.palaeo.2022.110860

Pereira, M.F. & Gama, C. 2017: Detrital provenance of the Upper Triassic siliciclastic rocks from southwest Iberia: a review. *Journal of Iberian Geology 43*, 379–393. https://doi.org/10.1007/s41513-017-0010-x

Pereira, M.F., Ribeiro, C., Gama, C., Drost, K., Chichorro, M., Vilallonga, F., Hofmann, M., & Linnemann, U. 2017: Provenance of upper Triassic sandstone, southwest Iberia (Alentejo and Algarve basins): tracing variability in the sources. *Geologische Rundschau 106*, 43–57. https://doi.org/10.1007/s00531-016-1295-2

Pérez-López, A. 1996: Sequence model for coastal-plain depositional systems of the Upper Triassic (Betic Cordillera, southern Spain). *Sedimentary Geology 101*, 99–117.

Pérez-López, A., Cambeses, A., Pérez-Valera, F. & Götz, A.E. 2021: Rhaetian tectono-magmatic evolution of the Central Atlantic

Magmatic Province volcanism in the Betic Cordillera, South Iberia. *Lithos 396–397*, 106230. https://doi.org/10.1016/j.lithos.2021.106230

Pérez-López, A., Pérez-Valera, F. & Götz, A. E. 2012: Record of epicontinental platform evolution and volcanic activity during a major rifting phase: The Late Triassic Zamoranos Formation (Betic Cordillera, S Spain). *Sedimentary Geology 247*, 39–57. https://doi.org/10.1016/j.sedgeo.2011.12.012

Pimentel, N.L., Wright, V.P., & Azevedo, T.M. 1996: Distinguishing early groundwater alteration effects from pedogenesis in ancient alluvial basins: examples from the Palaeogene of southern Portugal. *Sedimentary Geology 105*, 1–10. https://doi.org/10.1016/0037-0738(96)00034-6

Pla, C., Márquez-Aliaga, A. & Botella, H. 2013: The chondrichthyan fauna from the Middle Triassic (Ladinian) of the Iberian Range (Spain). *Journal of Vertebrate Paleontology 33*, 770–785. https://doi.org/10.1080/02724634.2013.748668

Platt, N.H. & Wright, V.P. 1992: Palustrine carbonates and the Florida Everglades; towards an exposure index for the fresh-water environment? *Journal of Sedimentary Research 62*, 1058–1071. https://doi.org/10.1306/D4267A4B-2B26-11D7-8648000102C1865D

Platt, N.H. & Wright, V.P. 2023: Flooding of a carbonate platform: The Sian Ka'an Wetlands, Yucatán, Mexico—a model for the formation and evolution of palustrine carbonate factories around the modern Caribbean Sea and in the depositional record. *The Depositional Record 9*, 99–151. https://doi.org/10.1002/dep2.217

Pommery, Y., Scheyer, T.M., Neenan, J.M., Reich, T., Fernandez, V., Voeten, D.F., Losko, A. S. & Werneburg, I. 2021: Dentition and feeding in Placodontia: tooth replacement in *Henodus chelyops*. *BMC Ecology and Evolution 21*, 1–19. https://doi.org/10.1186/s12862-021-01835-4

Popa, R., Kinkle, B.K., & Badescu, A. 2004: Pyrite Framboids as Biomarkers for Iron-Sulfur Systems. *Geomicrobiology Journal 21*, 193–206. https://doi.org/10.1080/01490450490275497

Pratsch, J.C. 1958: Stratigraphisch-tektonische Untersuchungen im Mesozoikum von Algarve (Sudportugal). *Geologisches Jahrbuch, Beihefte 30,* 1–123.

Preto, N., Kustatscher, E. & Wignall, P.B. 2010: Triassic climates — state of the art and perspectives. *Palaeogeography, Palaeoclimatology, Palaeoecology 290*, 1–10. https://doi.org/10.1016/j.palaeo.2010.03.015

Radley, J.D., & Coram, R.A. 2020: The earliest Laurasian unionoids? Freshwater bivalves from the Middle Triassic of Devon, southern UK. *Proceedings of the Geologists' Association*, *131*, 60–66. https://doi.org/10.1016/j.pgeola.2019.11.001

Rakshit, N. & Ray, S. 2021: Mortality dynamics and fossilisation pathways of a new metoposaurid-dominated multitaxic bonebed from India: a window into the Late Triassic vertebrate palaeoecosystem. *Historical Biology 33*, 2193–2215. https://doi.org/10.1080/08912963.2020.1777550

Ramos, A., Fernández, O., Terrinha, P., & Muñoz, J. A. 2016: Extension and inversion structures in the Tethys–Atlantic linkage zone, Algarve Basin, Portugal. *International Journal of Earth Sciences 105*, 1663–1679. https://doi.org/10.1007/s00531-015-1280-1

Reading, H.G. 1996: *Sedimentary Environments: Processes, Facies and Stratigraphy*. Wiley-Blackwell, Oxford.

Reineck, H.-E. & Wunderlich, F. 1968: Classification and Origin of Flaser and Lenticular Bedding. *Sedimentology 11*, 99–104. https://doi.org/10.1111/j.1365-3091.1968.tb00843.x

Reinhardt, L. & Ricken, W. 2000: The stratigraphic and geochemical record of Playa Cycles: monitoring a Pangaean monsoon-like system (Triassic, Middle Keuper, S. Germany). *Palaeogeography, Palaeoclimatology, Palaeoecology 161*, 205–227. https://doi.org/10.1016/S0031-0182(00)00124-3

Rinehart, L.F., Heckert, A.B., Hunt, A.P. & Spielmann, J.A. 2016: Rotten Hill: a Late Triassic bonebed in the Texas Panhandle, USA. *New Mexico Museum of Natural History & Science Bulletin* 72, 1–97.

Reolid, M., Muñiz Guinea, F., Toscano, A. & Belaústegui, Z. 2022: First record of fossil sauropterygians from the Upper Triassic of Southwestern Spain (Ayamonte, Huelva province). *Estudios Geológicos 78*. https://doi.org/10.3989/egeol.44639.613

Retallack, G.J. 1998: Core concepts of paleopedology. *Quaternary International 51*, 203–212. https://doi.org/10.1016/S1040-6182(97)00046-3

Retallack, G.J. 2008: *Soils of the Past: An Introduction to Paleopedology*. Wiley-Blackwell, Oxford.

Riding, J.B. 2021: A guide to preparation protocols in palynology. *Palynology 45,* 1–110. https://doi.org/10.1080/01916122.2021.1878305

Rocha, R.B. 1976: Estudo estratigráfico e paleontológico do Jurássico do Algarve Ocidental. *Ciências da Terra 2*, 1–178.

Rodrigues, B., Chew, D. M., Jorge, R.C.G.S., Fernandes, P., Veiga-Pires, C. & Oliveira, J.T. 2015: Detrital zircon geochronology of the Carboniferous Baixo Alentejo Flysch Group (South Portugal); constraints on the provenance and geodynamic evolution of the South Portuguese Zone. *Journal of the Geological Society 172*, 294–308. https://doi.org/10.1144/jgs2013-084

Rogers, R.R., Eberth, D.A., & Fiorillo, A.R. 2007: *Bonebeds: Genesis, Analysis, and Paleobiological Significance*. University of Chicago Press, Chicago.

Ronan, J., Duffin, C.J., Hildebrandt, C., Parker, A., Hutchinson, D., Copp, C. & Benton, M. J. 2020: Beginning of Mesozoic marine overstep of the Mendips: The Rhaetian and its fauna at Hapsford Bridge, Vallis Vale, Somerset, UK. *Proceedings of the Geologists' Association 131*, 578–594. https://doi.org/10.1016/j.pgeola.2020.02.005

Russel, D. & Russel, D. 1977: Premiers résultats d'une prospection paléontologique dans le Trias de l'Algarve (Portugal). *Ciências da Terra 3*, xx–xx.

Santos, A., Popovic, N. & Mayoral, E. 2022: Palaeoecology of Late Triassic marine assemblages from the proto-Atlantic Basin (Ayamonte, SW Spain). *Proceedings of the Geologists' Association 133*, 47–66. https://doi.org/10.1016/j.pgeola.2021.11.002

Sawlowicz, Z. 1993: Pyrite framboids and their development: a new conceptual mechanism. *Geologische Rundschau 82*, 148–156. https://doi.org/10.1007/BF00563277

Sawlowicz, Z. 2000: Framboids: from their origin to application. *Mineralogic Transactions 88*, 1–80.

Scheyer, T. M. 2007: Skeletal histology of the dermal armor of Placodontia: the occurrence of 'postcranial fibro-cartilaginous bone' and its developmental implications. *Journal of Anatomy 211*, 737–753. https://doi.org/10.1111/j.1469-7580.2007.00815.x

Scotese, C. & Schettino, A. 2017: Late Permian-Early Jurassic paleogeography of western Tethys and the world. *In:* Soto, J.I., Flinch, J.F. & Tari, G. (eds), *Permo-Triassic salt Provinces of Europe, North Africa and the Atlantic Margins*, 57–95. Elsevier, Amsterdam. https://doi.org/10.1016/B978-0-12-809417-4.00004-5

Sellwood, B.W. & Valdes, P.J. 2006: Mesozoic climates: general circulation models and the rock record. *Sedimentary Geology 190*, 269–287. https://doi.org/10.1016/j.sedgeo.2006.05.013

Shapiro, R.S., & Spangler, E. 2009: Bacterial fossil record in whale-falls: Petrographic evidence of microbial sulfate reduction. *Palaeogeography, Palaeoclimatology, Palaeoecology 274*, 196–203. https://doi.org/10.1016/j.palaeo.2009.02.006

Skawina, A. & Dzik, J. 2011: Umbonal musculature and relationships of the Late Triassic filibranch unionoid bivalves. *Zoological Journal of the Linnean Society 163*, 863–883. https://doi.org/10.1111/j.1096-3642.2011.00728.x

Smith, L.M. 2003: *Playas of the Great Plains*. University of Texas Press, Austin.

Soares, A., Marques, J. & Sequeira, A. 2007: Carta Geológica de Portugal na escala 1: 50000. *Notícia explicativa da folha 19.*

Soares, A.F., Kullberg, J.C., Marques, J.F., da Rocha, R.B. & Callapez, P.M. 2012: Tectono-sedimentary model for the evolution of the Silves Group (Triassic, Lusitanian basin, Portugal). *Bulletin*

*de la Société G*éologique de France 183, 203–216. https://doi.org/10.2113/gssgfbull.183.3.203

Stocker, M.R. & Butler, R.J. 2013: Phytosauria. *Geological Society, London, Special Publications*, *379*, 91–117.

Stocker, M.R., Zhao, L.-J., Nesbitt, S.J., Wu, X.-C. & Li, C. 2017: A short-snouted, Middle Triassic phytosaur and its implications for the morphological evolution and biogeography of Phytosauria. *Scientific Reports 7*, 46028. https://doi.org/10.1038/srep46028

Suárez, J. 2007: La Mancha Triassic and Lower Lias Stratigraphy, a well log interpretation. *Journal of Iberian Geology 33*, 55–78.

Sues, H.D. & Fraser, N.C. 2010: *Triassic Life on Land: the Great Transition*. Columbia University Press, New York.

Sulpis, O., Agrawal, P., Wolthers, M., Munhoven, G., Walker, M. & Middelburg, J.J. 2022: Aragonite dissolution protects calcite at the seafloor. *Nature Communications 13*, 1104. https://doi.org/10.1038/s41467-022-28711-z

Szulc, J., Racki, G., Jewuła, K. & Srodon, J. 2015: How many Upper Triassic bone-bearing levels are there in Upper Silesia (southern Poland)? A critical overview of stratigraphy and facies. *Annales Societatis Geologorum Poloniae 85*, 587–626. https://doi.org/10.14241/asgp.2015.037

Tabor, N.J. & Myers, T.S. 2015: Paleosols as indicators of paleoenvironment and paleoclimate. *Annual Review of Earth and Planetary Sciences 43*, 333–361. https://doi.org/10.1146/annurev-earth-060614-105355

Tanner, L.H. 2018: Climates of the Late Triassic: perspectives, proxies and problems. *In:* Tanner, L.H. (ed.), *The Late Triassic World: Earth in a Time of Transition,* 59–90. Springer International Publishing, Dordrecht. https://doi.org/10.1007/978-3-319-68009-5_3

Tanner, S. & Lucas, L. 2006: Calcareous paleosols of the Upper Triassic Chinle Group, Four

Corners region, southwestern United States: Climatic implications. *Geological Society of America Special Paper 416*, 53–74. https://doi.org/10.1130/2006.2416(04)

Teixeira, C. 1942: Notas sobre a Geologia do Triassico Português. *Boletim da Sociedade Geológica de Portugal 1*, 161–174.

Teixeira, C. 1948: *Flora Mesozóica Portuguesa*. Direcção Geral de Minas e Serviços Geológicos, Serviços Geológicos de Portugal, Lisbon.

Terrinha, P., Kullberg, J. C., Neres, M., Alves, T., Ramos, A., Ribeiro, C., Mata, J., Pinheiro, L., Afilhado, A., Matias, L., Luís, J., Muñoz, J. A., & Fernández, Ó. 2019: Rifting of the southwest and west Iberia continental Margins. In: Quesada, C. & Oliveira, J. (eds), *The Geology of Iberia: A Geodynamic Approach. Regional Geology Reviews*. Springer Cham, 251–283. https://doi.org/10.1007/978-3-030-11295-0_6

Terrinha, P., Rocha, R.B, Rey, J., Cachão, M., Moura, D., Roque, C., Martins, L., Valadares, V., Cabral, J., Azevedo, M.R., Barbero, L., Clavijo, E., Dias, R.P., Matias, H., Madeira, J., Silva, C.M., Munhá, J., Rebelo, L., Ribeiro, C., Vicente, J., Noiva, J., Youbi, N., & Bensalah, M.K. 2006: A Bacia do Algarve: Estratigrafia, Paleogeografia e Tectónica. *In: Geologia de Portugal no contexto da Ibéria.* Universidade de Évora, Évora.

Tinterri, R. 2011: Combined Flow Sedimentary Structures and the Genetic Link Between Sigmoidal- and Hummocky-Cross Stratification. *GEOACTA 10*, 1–43.

Trindade, M.J., Rocha, F. & Dias, M.I. 2010: Geochemistry and mineralogy of clays from the Algarve Basin, Portugal: a multivariate approach to palaeoenvironmental investigations. *Current Analytical Chemistry 6*, 43–52. https://doi.org/10.2174/157341110790069682

Tucker, M. 2001: *Sedimentary Petrology – An Introduction to the Origin of Sedimentary Rocks*. Blackwell Scientific Publications, London.

Turner, P. 1980: *Continental Red Beds*. Elsevier, Amsterdam.

van Hinsbergen, D.J.J., de Groot, L.V., van Schaik, S.J., Spakman, W., Bijl, P.K., Sluijs, A., Langereis, C.G. & Brinkhuis, H. 2015: A paleolatitude calculator for paleoclimate studies. *PLoS One 10*, e0126946. https://doi.org/10.1371/journal.pone.0126946

Verati, C., Rapaille, C., Féraud, G., Marzoli, A., Bertrand, H. & Youbi, N. 2006: $^{40}Ar/^{39}Ar$ ages and duration of the Central Atlantic Magmatic Province volcanism in Morocco and Portugal and its relation to the Triassic–Jurassic boundary. *Palaeogeography, Palaeoclimatology, Palaeoecology 244*, 308-325. https://doi.org/10.1016/j.palaeo.2006.06.033

Vieira, F.V., Bastos, A.C., Quaresma, V.S., Leite, M.D., Costa, A., Oliveira, K.S.S., Dalvi, C.F., Bahia, R.G., Holz, V.L., Moura, R.L, & Amado Filho, G.M. 2019: Along-shelf changes in mixed carbonate-siliciclastic sedimentation patterns. *Continental Shelf Research 187*, 103964. https://doi.org/10.1016/j.csr.2019.103964

Vilas-Boas, M. 2023: *Palynology of the Triassic: Jurassic of the Silves Group in Portugal, its Implications on a Changing World*. Unpublishedf PhD dissertation, Laboratorio Nacional de Energia e Geologia, Portugal.

Vilas-Boas, M., Paterson, N. W., Pereira, Z., Fernandes, P. & Cirilli, S. 2022: The age of the first pulse of continental rifting associated with the breakup of Pangea in Southwest Iberia: new palynological evidence. *Journal of Iberian Geology 48*, 181–190. https://doi.org/10.1007/s41513-022-00189-0

Vilas-Boas, M., Pereira, Z., Cirilli, S. & Fernandes, P. 2024: New Insights on the Upper Triassic Silves Group in Algarve Basin, Portugal: Palynological, paleophytogeography and paleoclimatology advances. *Geobios 86,* 49–64. https://doi.org/10.1016/j.geobios.2024.08.001

Visser, M.J. 1980: Neap-spring cycles reflected in Holocene subtidal large-scale bedform deposits: a preliminary note. *Geology 8*, 543–546. https://doi.org/10.1130/0091-7613(1980)8<543:NCRIHS>2.0.CO;2

Vollmer, T., Werner, R., Weber, M., Tougiannidis, N., Röhling, H.-G. & Hambach, U. 2008: Orbital control on Upper Triassic Playa cycles of the Steinmergel-Keuper (Norian): a new concept for ancient playa cycles. *Palaeogeography, Palaeoclimatology, Palaeoecology 267*, 1–16. https://doi.org/10.1016/j.palaeo.2007.12.017

von Huene, F. 1936: *Henodus chelyops*, ein neuer Placodontier. *Palaeontographica Abteilung A*, 99–147.

von Huene, F. 1938: Der dritte *Henodus*. Ergänzungen zur Kenntnis des Placodontiers *Henodus chelyops* Huene. *Palaeontographica Abteilung A*, 105–115.

Wang, P. 2012: Principles of Sediment Transport Applicable in Tidal Environments. In: Davis, R. Jr. & Dalrymple, R. (eds), *Principles of Tidal Sedimentology*. Springer Dordrecht, 19–34. https://doi.org/10.1007/978-94-007-0123-6_2

Watts, N. 1978: Displacive calcite: evidence from recent and ancient calcretes. *Geology 6*, 699–703.

Wignall, P.B., & Atkinson, J.W. 2020*:* A two-phase end-Triassic mass extinction. *Earth-Science Reviews 208*, 103282. https://doi.org/10.1016/j.earscirev.2020.103282

Witzmann, F. & Gassner, T. 2008*:* Metoposaurid and mastodonsaurid stereospondyls from the Triassic–Jurassic boundary of Portugal. *Alcheringa 32*, 37–51. https://doi.org/10.1080/03115510701757316

Wright, V.P. & Tucker, M.E. 2009: *Calcretes*. Wiley-Blackwell, Chichester.

Youbi, N., Martins, L.T., Munhá, J.M., Ibouh, H., Madeira, J., Aït Chayeb, E.H. & El Boukhari, A. 2003: The Late Triassic-Early Jurassic Volcanism of Morocco and Portugal in the Framework of the Central Atlantic Magmatic Province. *In:* Hames, W.E., McHone, J.M., Renne, P.R. & Ruppel, C. (eds), *The Central Atlantic Magmatic Province: Insights from Fragments of Pangea*. American Geophysical Union Monograph 136, 179–207. https://doi.org/10.1029/136GM010

Zhang, J. 2007: Two shark finspines (Hybodontoidea) from the Mesozoic of North China. *Cretaceous Research 28*, 277–280. https://doi.org/10.1016/j.cretres.2006.05.005